Why Does Risk Matter More in Recessions than in Expansions?*

Martin M. Andreasen† Giovanni Caggiano‡

Efrem Castelnuovo§ Giovanni Pellegrino¶

August 2021

Abstract

This paper uses a nonlinear vector autoregression and a non-recursive identification strategy to show that an equal-sized uncertainty shock generates a larger contraction in real activity when growth is low (as in recessions) than when growth is high (as in expansions). An estimated New Keynesian model with recursive preferences and approximated to third order around its risky steady state replicates these state-dependent responses. The key mechanism behind this result is that firms display a stronger upward nominal pricing bias in recessions than in expansions, because recessions imply higher inflation volatility and higher marginal utility of consumption than expansions.

Keywords: New Keynesian Model, Nonlinear SVAR, Non-recursive identification, State-dependent uncertainty shock, Risky steady state.

*We thank Guido Ascari, Nicholas Bloom, Ryan Chahrour, Chris Edmond, Andrea Ferrero, Pablo Guerron-Quintana, Tom Holden, Michel Juillard, Martin Kleim, Sydney Ludvigson, Elmar Mertens, Juan Rubio-Ramirez, Henning Weber and participants to many seminar and conference audiences for their comments. Andreasen and Pellegrino acknowledge funding from the Independent Research Fund Denmark, project number 7024-00020B. Caggiano and Castelnuovo acknowledge financial support by the Australian Research Council (respectively, DP190102802 and DP160102281). .

†Aarhus University, CREATES, and the Danish Finance Institute. Email: mandreasen@econ.au.dk.

‡Monash University and University of Padova. Email: giovanni.caggiano@monash.edu.

§University of Padova. Email: efrem.castelnuovo@unipd.it.

¶Aarhus University. Email: gpellegrino@econ.au.dk.

1 Introduction

The Great Recession and the recent COVID-19 pandemic have gone hand-in-hand with spectacular spikes in virtually all measures of US uncertainty (Bloom (2014), Barrero and Bloom (2020)). Following the seminal papers by Bloom (2009) and Fernández-Villaverde et al. (2011), numerous studies have investigated the importance of uncertainty shocks for the business cycle. This paper makes three contributions to this literature. First, using a nonlinear vector autoregressive (VAR) with a non-recursive identification strategy, we show that an equal-sized uncertainty shock generates a larger contraction in real activity when growth is low (as in recessions) than when growth is high (as in expansions). Second, we demonstrate that a dynamic stochastic general equilibrium (DSGE) model approximated to third order around its risky steady state is able to capture such state-dependent responses to an uncertainty shock. In contrast, any state-dependent effects of this shock are absent when using the deterministic steady state for the third-order approximation, as commonly done in the literature. Third, relying on this methodological contribution, we use an estimated New Keynesian model to examine the economic mechanisms behind our new VAR evidence. The results reveal that the traditional aggregate supply (AS) relation implies an upward nominal pricing bias for firms, as emphasized in Fernández-Villaverde et al. (2015), but that this bias is *state-dependent* and essential to understand the asymmetric responses to an uncertainty shock. As a result, our analysis delivers an empirically credible micro-founded model that can be used to study the role of monetary policy for addressing the state-dependent effects of uncertainty shocks across the business cycle.

Let us elaborate on our contributions. First, we estimate a nonlinear VAR using quarterly US data to assess whether an uncertainty shock has real effects that depend on the stance of the business cycle. To allow for potentially state-dependent effects to a shock, we extend the standard VAR by adding quadratic terms that involve the growth rate of real GDP and a proxy for financial uncertainty, which are both endogenous in the VAR. Uncertainty shocks are identified using a non-recursive strategy that combines event, correlation, and sign restrictions following the recent work of Antolín-Díaz and Rubio-Ramírez (2018) and Ludvigson et al. (2019). Our main empirical result is that an uncertainty shock of the same size generates a larger response of real activity during recessions than in expansions. This finding is in line with previous contributions on the nonlinear effects of uncertainty shocks (see, for instance, Caggiano et al. (2014), Alessandri and Mumtaz (2019), Cacciatore and Ravenna (2020)). Importantly, our empirical finding is based on a non-recursive identification strategy, and is therefore not subject to the critique in Ludvigson et al. (2019) of the standard recursive identification scheme

often used to identify exogenous variations in uncertainty.

Our second contribution is methodological and relates to the ability of nonlinear DSGE models to generate state-dependent effects of uncertainty shocks. These models are widely used in the literature to study the economic mechanisms behind the real effects of uncertainty shocks when solved by a third-order approximation around the deterministic steady state, as in Fernández-Villaverde et al. (2011), Born and Pfeifer (2014), Fernández-Villaverde et al. (2015), and Basu and Bundick (2017), among many others. This is a fruitful way to proceed to understand the effects of uncertainty shocks *on average*. However, it does not allow the researcher to investigate the potentially *state-dependent* effects of uncertainty shocks, because only the level of a given variable and terms that are linear in the states are risk-corrected in this approximation (Cacciatore and Ravenna (2020)). One way to address this shortcoming is to apply a fourth-order approximation around the deterministic steady state, because it also corrects terms that are quadratic in the states and hence allows for state-dependent effects of uncertainty shocks, as exploited in Cacciatore and Ravenna (2020) and Diercks et al. (2020). But going beyond a third-order approximation substantially increases the execution time and the memory requirement when solving DSGE models, which may limit the applicability of this solution when the desire is to formally estimate these models. We therefore propose a computationally less demanding alternative by simply moving the approximation point for the third-order approximation to the risky steady state.[1] This long-term equilibrium point is characterized by allowing agents to respond to uncertainty, whereas any effects of uncertainty is absent in the deterministic steady state. The appealing feature of this modification is that all linear *and* nonlinear terms in the approximation are adjusted for risk, enabling us to capture potentially different effects of uncertainty shocks in expansions and recessions. To ensure stability, we also provide a pruned version of this approximation and its closed-form solution for unconditional first and second moments as well as impulse response functions by using the results in Andreasen et al. (2018). Hence, our contribution makes it feasible to estimate nonlinear DSGE models with state-dependent effects of uncertainty shocks using techniques that are commonly applied in the literature.

Building on this methodological contribution, in the third part of the paper we work with a version of the New Keynesian model proposed by Basu and Bundick (2017) and refined in Basu and Bundick (2018) to understand why risk matters more in recessions than in expansions. Key features of this model are recursive preferences as in Epstein and Zin (1989), an uncertainty shock in the disturbance to the household's utility function, and nominal price stickiness as in Rotemberg (1982). We extend the model by consumption habits, the flexible formulation of recursive preferences in Andreasen and Jørgensen

[1] Solutions around the risky steady state are discussed in Coeurdacier et al. (2011) for a first-order approximation and in de Groot (2013) for approximations up to second order. However, the methods adopted in these papers to compute approximations around the risky steady state differ from the approach applied in the present paper.

(2020), and cost-push shocks. This model is then estimated by matching stylized unconditional moments jointly with our nonlinear VAR impulse response functions to an uncertainty shock in both recessions and expansions. The estimation results show that this New Keynesian model goes a long way in reproducing the different responses to uncertainty shocks in expansions and recessions. Crucially, these differences in the impulse response functions arise from different initial conditions as captured by different values of the states, which through the model's endogenous propagation mechanisms make uncertainty shocks more severe in recessions than in expansions. In other words, we do not rely on any form of occasionally binding constraints as in Cacciatore and Ravenna (2020) or an unanticipated switch in the structural parameters attached to different subsamples to generate asymmetric responses to uncertainty shocks. A further investigation of the model reveals that these asymmetries are primarily generated by the nonlinear terms in the aggregate supply (or Phillips) curve that lead firms to set higher nominal prices than what would be optimal without uncertainty. Hence, our results show that in response to an uncertainty shock firms bias their prices upward relatively more in recessions than in expansions, and therefore display a *state-contingent upward nominal pricing bias*. To understand this effect, recall that firms can reset their prices in every period with sticky prices as in Rotemberg (1982) but they face costs when doing so. In this setting, the conditional volatility of inflation affects the current price, because it is optimal for firms to set higher prices after an uncertainty shock to avoid large expensive future increases in prices. That is, firms simply smooth out their pricing bias. Two effects help to make this pricing bias stronger in recessions than expansions. First, inflation volatility is higher in recessions than in expansions. Second, firms discount future profits by the consumption-based stochastic discount factor, which has a higher level in recessions than in expansions due to lower consumption and higher marginal utility when growth is low. This implies that firms assign more weight to future profits in recessions, which also help to increase their pricing bias. We finally show that this explanation of a state-contingent upward nominal pricing bias is consistent with evidence for firms' price markup, which increases by more in recessions than in expansions following an uncertainty shock.

The rest of this paper is organized as follows. Section 2 provides VAR evidence on the effects of uncertainty shocks, while Section 3 presents an otherwise standard New Keynesian model with recursive preferences. The proposed model solution is described in Section 4, and we discuss our empirical findings for the New Keynesian model in Section 5. Section 6 investigates the key mechanism behind the state-dependent effects of uncertainty shocks. Concluding comments are provided in Section 7.

2 VAR Evidence

This section presents our reduced-form evidence for state-dependent effects of an uncertainty shock. We introduce a nonlinear VAR in Section 2.1, discuss identification in Section 2.2, and present the impulse responses in Section 2.3. Various robustness checks are discussed in Section 2.4, while Section 2.5 presents a simulation study that validates the applied estimation method.

2.1 An Interacted VAR

We consider the vector of macro variables $\mathbf{Y}_t = [\log VXO_t, \log GDP_t, \log C_t, \log I_t, \log H_t, \log P_t, R_t]'$ of dimension $n \times 1$, where VXO_t is the implied volatility index in the stock market (the S&P 100), GDP_t is output, C_t is consumption, I_t is investment, H_t is hours worked, P_t is the price level, and R_t is the policy rate.[2] The vector $\mathbf{Y}_t$ evolves as specified by the following interacted VAR (IVAR)

$$\mathbf{Y}_t = \boldsymbol{\alpha} + \sum_{j=1}^{L} \mathbf{A}_j \mathbf{Y}_{t-j} + \sum_{j=1}^{L} \mathbf{c}_j \log VXO_{t-j} \times \Delta \log GDP_{t-j} + \boldsymbol{\eta}_t, \tag{1}$$

where $\boldsymbol{\alpha}$ and $\mathbf{c}_j$ have dimension $n \times 1$, $\mathbf{A}_j$ has dimension $n \times n$, and the $n \times 1$ vector of residuals $\boldsymbol{\eta}_t \sim \mathcal{IID}(\mathbf{0}, \boldsymbol{\Omega})$. Unlike linear VARs, our IVAR includes the quadratic terms $\log VXO_{t-j} \times \Delta \log GDP_{t-j}$ to capture potentially state-contingent effects of higher uncertainty for various levels of the growth rate in GDP, i.e., $\Delta \log GDP_t \equiv \log(GDP_t/GDP_{t-1})$. We estimate this IVAR with four lags by OLS using quarterly US data from 1962Q3 to 2017Q4.[3] Given that the VXO is unavailable before 1986, we follow Bloom (2009) and combine the VXO by the monthly volatility of daily returns in the S&P 500 before 1986. Our sample includes the zero lower bound for the monetary policy rate from 2008Q4 to 2015Q4. Hence, we replace the federal funds rate in this period by the shadow rate of Wu and Xia (2016) to account for unconventional monetary policy. The estimation results clearly favor our IVAR specification against a linear VAR, as we reject the joint null hypothesis of $\mathbf{c}_j = 0$ for $j = \{1, 2, 3, 4\}$ with a likelihood ratio test statistics of 62.0, implying a p-value of 0.0002 in the χ^2_{28}-distribution. Table 1 reports stylized unconditional moments for the growth rates of the four variables in the VAR and IVAR that are related to economic activity. Both models match the empirical means and standard deviations, and hence show no sign of overfitting. We also see that the IVAR is marginally

[2] The definition of these variables follows the one used by Basu and Bundick (2017) for their VAR.

[3] Alternatives to the IVAR include the nonlinear factor model in Guerron-Quintana et al. (2021) and the quadratic autoregression in Aruoba et al. (2017) that both are motivated from a second-order pruned perturbation approximation. We prefer the IVAR because it is computationally easier to estimate than the factor model in Guerron-Quintana et al. (2021), which requires the use of a particle filter. To our knowledge, the quadratic autoregression in Aruoba et al. (2017) is currently only developed for univariate time series.

better at generating negative skewness and excess kurtosis than the linear VAR. Thus, the presence of nonlinear terms allow the IVAR to better capture higher order moments of the empirical distribution than implied by the linear VAR.

Table 1: VARs: Unconditional Moments for Economic Activity
This table reports unconditional moments for the growth rate in output, consumption, investment, and hours worked using US data from 1962Q3 to 2017Q4. The corresponding moments in the linear VAR and the IVAR are obtained from 500 simulated time series of the same lenght as in the empirical sample.

	Data				Linear VAR				IVAR			
	Mean	Std.	Skew.	Kurt.	Mean	Std.	Skew.	Kurt.	Mean	Std.	Skew.	Kurt.
Growth rates:												
Output	0.39	0.81	-0.36	4.75	0.38	0.81	-0.004	3.23	0.38	0.81	-0.02	3.30
Consumption	0.40	0.46	-0.27	4.01	0.39	0.45	-0.09	3.20	0.39	0.45	-0.13	3.20
Investment	0.69	2.06	-1.15	6.70	0.63	2.07	-0.13	3.52	0.64	2.00	-0.26	3.73
Hours worked	0.04	0.66	-0.92	5.18	0.04	0.66	-0.02	3.10	0.04	0.63	-0.26	3.50

2.2 Uncertainty Shocks: Identification Strategy

Following Bloom (2009), many contributions in the literature have identified uncertainty shocks by imposing zero-restrictions either on the impact of macroeconomic shocks on uncertainty or on the impact of uncertainty shocks on the business cycle. However, this recursive identification strategy has recently been questioned by Ludvigson et al. (2019), who find a non-zero contemporaneous correlation between uncertainty and the business cycle. We therefore follow Ludvigson et al. (2019) and use a combination of event restrictions and constraints from external variables, which we supplement with sign restrictions to obtain a robust non-recursive identification of uncertainty shocks. To present this alternative, let $\mathbf{e}_t$ denote the structural shocks with zero mean and covariance matrix $\mathbf{I}_n$. The mapping between the reduced-form residuals $\boldsymbol{\eta}_t$ and the structural shocks $\mathbf{e}_t$ in the IVAR is $\boldsymbol{\eta}_t = \boldsymbol{B}\mathbf{e}_t$, where $\boldsymbol{B} = \boldsymbol{P}\boldsymbol{Q}$ is of dimension $n \times n$, $\boldsymbol{P}$ is a lower-triangular Cholesky factor of $\boldsymbol{\Omega}$ with non-negative diagonal elements, and $\boldsymbol{Q}$ is any orthonormal rotation matrix (i.e., $\boldsymbol{Q}\boldsymbol{Q}' = \boldsymbol{I_n}$) that implies positive diagonal elements of $\boldsymbol{B}$. Let $\mathcal{B}$ denote the set that contains the infinitely many solutions of $\boldsymbol{B}$ that satisfy the $n(n+1)/2$ restrictions implied by the covariance matrix, i.e., $\boldsymbol{\Omega} = \boldsymbol{B}\boldsymbol{B}'$. Given that not all of these mathematically acceptable solutions are interesting from an economic standpoint, we impose restrictions to get the subset of economically admissible solutions.[4]

[4]The set $\mathcal{B}$ is constructed using the algorithm in Rubio-Ramírez et al. (2010). First, we initialize $\boldsymbol{B}$ to be the unique lower-triangular Cholesky factor $\boldsymbol{P}$. Then, we rotate $\boldsymbol{B}$ by drawing $K = 500,000$ random orthogonal matrices $\boldsymbol{Q}$. Each rotation is performed by drawing an $n \times n$ matrix $\boldsymbol{M}$ from a $\mathcal{N}(0, \boldsymbol{I_n})$ density. Then, $\boldsymbol{Q}$ is taken to be the orthonormal matrix in the $\boldsymbol{QR}$ decomposition of $\boldsymbol{M}$. Let $\boldsymbol{e}_t(\boldsymbol{B}) =$

The first set of restrictions we impose relate to specific events or narratives following the work of Antolín-Díaz and Rubio-Ramírez (2018) and Ludvigson et al. (2019). In particular, we consider the dates located by Bloom (2009) that coincide with spikes in the financial uncertainty proxy of Ludvigson et al. (2019).[5] In addition, we also include the events emphasized in Ludvigson et al. (2019) as well as 2000Q2 (collapse of the dot-com bubble) and 2010Q2 (Euro area debt crisis and fears about a global slowdown) with clear spikes in the financial uncertainty proxy of Ludvigson et al. (2019). At each of the dates, we require that realized uncertainty shocks $e_{unc,t}$ exceed their 50th percentile $p\left(e_{unc,t}, 50\right)$ across all unconstrained solutions in $\mathcal{B}$, except on 1987Q4 (Black Monday) and 2008Q4 (collapse of Lehman Brothers) where the uncertainty shock should exceed its 75th percentile as in Ludvigson et al. (2019). The selected dates with spikes in financial uncertainty are plotted in Figure 1.

Figure 1: Spikes in Financial Uncertainty

The red line denotes financial volatility according to the VXO since 1986, and the realized volatility in the S&P 500 before 1986 as in Bloom (2009). The blue line is the measure of financial uncertainty in Ludvigson et al. (2019) for a forecast horizon of one month. Vertical black lines denote the events that are used to identify uncertainty shocks as reported in Table 2.

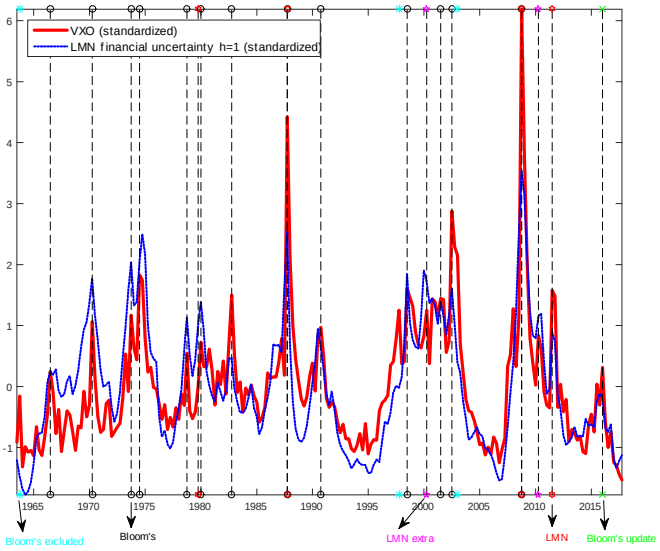

Our second set of restrictions impose two external constraints on $e_{unc,t}$ following the work of Ludvigson et al. (2019). The first requirement is that the correlation between $e_{unc,t}$ and the stock market return R_t^m must be lower than the median value of this correlation

$\boldsymbol{B}_t^{-1}\boldsymbol{\eta}_t$ be the shocks implied by $\boldsymbol{B} \in B$ for a given $\boldsymbol{\eta}_t$. Then, K different matrices $\boldsymbol{B}$ imply K different unconstrained shocks $\boldsymbol{e}_t(\boldsymbol{B}) = \boldsymbol{B}^{-1}\boldsymbol{\eta}_t$, $t = 1, ..., T$.

[5] When examining the recent peaks in the VXO, we identify one in 2016Q1, which we also include. Several uncertainty-triggering events occurred right before or during this quarter, e.g., the first increase of the federal funds rate that ended the zero lower bound phase after seven years; fears about China's economic fragility; the policy rate in Japan became negative; and the announcement in February 2016 by the British Prime Minister David Cameron of the Brexit referedum in June that year.

across all unconstrained solutions in $\mathcal{B}$. In our case, this implies that the correlation between R_t^m and $e_{unc,t}$ must be less than or equal to -0.15, which is a stronger requirement than imposed in Ludvigson et al. (2019). The motivation for this assumption is the well-known leverage effect, which implies that a negative shock to the stock market (that reduces R_t^m) make firms more leveraged and hence more risky. The second constraint requires that the correlation between $e_{unc,t}$ and the growth rate in the real gold price Δg_t must be higher than the median value of this correlation across all unconstrained solutions in $\mathcal{B}$. In our case, this means that the correlation between Δg_t and $e_{unc,t}$ must be bigger than or equal to 0.03, which also is slightly more restrictive than in Ludvigson et al. (2019). The theoretical justification for this constraint is that gold operates as a safe asset among investors, and its price should therefore be positively correlated with uncertainty shocks due to higher demand.

To further sharpen the identification, we require a non-positive response of GDP, investment, consumption, and hours on impact following a positive uncertainty shock, which is consistent with a large number of theoretical and empirical investigations of uncertainty shocks (see, e.g., Bloom (2014) for a survey). As shown in the Online Appendix, these sign restrictions only help to narrow the identified set but have hardly any effect on the median target of the identified set, which we will focus on in our subsequent analysis. For completeness, all the identification restrictions are summarized in Table 2.

2.3 Impulse Response Functions

We quantify the business cycle effects of uncertainty shocks by computing generalized impulse response functions (GIRFs) that account for the nonlinearities introduced by the term $\log VXO_{t-j} \times \Delta \log GDP_{t-j}$ in the IVAR (Koop et al. (1996)). The GIRFs for $\mathbf{Y}_t$ at horizon h to an uncertainty shock of size δ_{unc} in period t is defined as

$$GIRF_{\mathbf{Y}}(h, \delta_{unc}, \boldsymbol{\varpi}_{t-1}) \equiv \mathbb{E}\left[\mathbf{Y}_{t+h} | \delta_{unc}, \boldsymbol{\varpi}_{t-1}\right] - \mathbb{E}\left[\mathbf{Y}_{t+h} | \boldsymbol{\varpi}_{t-1}\right]. \tag{2}$$

These impulse responses depend on the state of the economy, which is captured by the initial conditions $\boldsymbol{\varpi}_{t-1} \equiv \{\mathbf{Y}_{t-1}, ..., \mathbf{Y}_{t-L}\}$. We are interested in exploring the effects of an uncertainty shock across the business cycle, and we therefore compute GIRFs when the initial condition for real GDP growth is below its $10th$ percentile (i.e., deep recessions) and above its $90th$ percentile (i.e., strong expansions). The results are reported in the left column in Figure 2, which shows the responses for the the median target (MT) model $\boldsymbol{B_{MT}}$, which is the solution in $\mathcal{B}$ that delivers the GIRFs with the smallest distance to the median of the impulse responses in the identified set (see Fry and Pagan (2011)). For a positive one-standard deviation uncertainty shock ($\delta_{unc} = 1$), we find the familiar drop in real activity for several quarters after the shock in both recessions and expansions. However, the key focus of the present paper is the finding that this drop in activity

Table 2: Identifying Restrictions for Uncertainty Shocks

This table summarizes the identifying assumptions for uncertainty shocks in the IVAR. For event restrictions, the notation $\geqslant p(e_{Unc,t}, 50^{th})$ indicates that the uncertainty shock at a given date should exceed the 50^{th} percentile of its distribution. The sources for each of these event constraints are from Bloom (2009) and Ludvigson et al. (2019) (LMN). Excluded dates from Bloom (2009) are 1963Q4 (Assassination of JFK), 1997Q4 (Asian crisis), and 2003Q1 (Iraq invasion).

	Conditions on $e_{unc,t}$	Source
Event Restrictions		
1966Q3: Vietnam buildup	$\geqslant p(e_{unc,t}, 50^{th})$	Bloom
1970Q2: Cambodia and Kent state	$\geqslant p(e_{unc,t}, 50^{th})$	Bloom
1973Q4: OPEC I, Arab-Israeli War	$\geqslant p(e_{unc,t}, 50^{th})$	Bloom
1974Q3: Franklin National	$\geqslant p(e_{unc,t}, 50^{th})$	Bloom
1978Q4: OPEC II	$\geqslant p(e_{unc,t}, 50^{th})$	Bloom
1979Q4: Volcker experiment	$\geqslant p(e_{unc,t}, 50^{th})$	LMN
1980Q1: Afghanistan, Iran hostages	$\geqslant p(e_{unc,t}, 50^{th})$	Bloom
1982Q4: Monetary policy turning point	$\geqslant p(e_{unc,t}, 50^{th})$	Bloom
1987Q4: Black Monday	$\geqslant p(e_{unc,t}, 75^{th})$	Bloom & LMN
1990Q4: Gulf War I	$\geqslant p(e_{unc,t}, 50^{th})$	Bloom
1998Q3: Russian, LTCM default	$\geqslant p(e_{unc,t}, 50^{th})$	Bloom
2000Q2: Collapse of the tech bubble	$\geqslant p(e_{unc,t}, 50^{th})$	LMN extra
2001Q3: 9/11 terrorist attacks	$\geqslant p(e_{unc,t}, 50^{th})$	Bloom
2002Q3: Worldcom, Enron	$\geqslant p(e_{unc,t}, 50^{th})$	Bloom
2008Q4: Great recession	$\geqslant p(e_{unc,t}, 75^{th})$	Bloom & LMN
2010Q2: European debt crisis	$\geqslant pe_{unc,t}, 50^{th})$	LMN extra
2011Q3: Debt ceiling crisis	$\geqslant p(e_{unc,t}, 50^{th})$	LMN
2016Q1: FFR liftoff and China	$\geqslant p(e_{unc,t}, 50^{th})$	Bloom (update)
External Restrictions		
Stock market return, r_t^m	$\leqslant p(corr(e_{unc,t}, r_t^m), 50^{th})$	LMN
Real log difference price of gold, Δg_t	$\geqslant p(corr(e_{unc,t}, \Delta g_t), 50^{th})$	LMN
S*ign Restrictions on Impact*		
GDP	< 0	
Investment	< 0	
Consumption	< 0	
Hours	< 0	

is *larger* and *more persistent* in deep recessions (the red dotted lines) than in strong expansions (the blue lines) although the size of the uncertainty shock is the same. For instance, in recessions the peak responses of output, investment, and hours are -0.28%, -0.87%, and -0.45%, respectively, whereas the corresponding responses in expansions are only -0.19%, -0.35%, and -0.23%. Turning to the nominal side, the responses for prices are slightly positive in expansions and slightly negative in recessions. For the monetary policy rate, we find a clear negative effect of an uncertainty shock, with effects that are stronger in recessions than in expansions.

Figure 2: Nonlinear VAR: Impulse Responses to an Uncertainty Shock
The charts to the left show the median target responses in the IVAR in deep recessions and strong expansions following a positive one-standard deviation uncertainty shock. The charts to the right show the difference between these responses in (deep recessions minus strong expansions) in addition to the 68 and 90 percent confidence interval, which are estimated by a residual-based bootstrap (with 1,000 draws) when conditioning on the median target responses. All responses are shown in percentage deviations, except for the policy rate where changes in percentage points are reported.

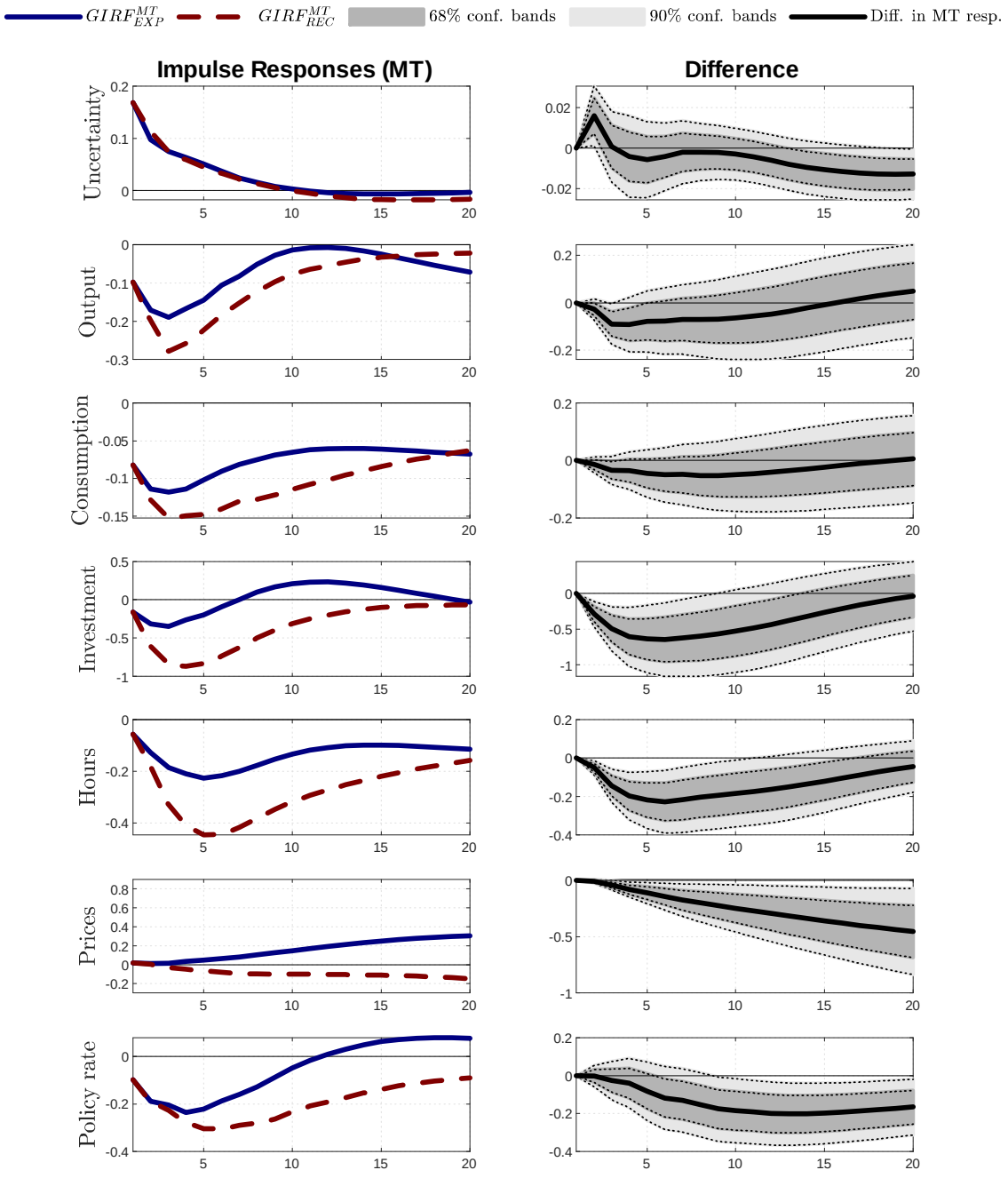

The charts to the right in Figure 2 report the distance between the MT responses in recessions relative to the MT responses in expansions, where the shaded gray and

light gray areas report the bootstrapped 68% and 90% confidence intervals, respectively.[6] These confidence intervals reveal that the different responses in expansions and recessions in general are significant at the 68% level, and for investment, hours, prices, and the policy rate we even have significance at the 90% level.

2.4 Robustness Analysis

In the Online Appendix, we show that our new result is robust to the following modifications and extensions of the IVAR presented above: i) re-estimating the IVAR using data from 1987Q1 to 2017Q4 to only use the official VXO measure and to exclude the Great Inflation period; ii) replacing the shadow rate of Wu and Xia (2016) by the federal funds rate throughout the sample and adding the 10-year Treasury zero-coupon yield to capture effects of quantitative easing and forward guidance; iii) adding a series for realized skewness in the S&P500 to control for skewness shocks as discussed in Salgado et al. (2019); iv) use the purchasing managers index instead of real GDP growth for the interactive term in the IVAR; v) controlling for first-moment financial shocks by including the credit spread between BAA and AAA yields for bonds with more than 20 years to maturity; and vi) defining the expansionary state as episodes where real GDP growth is above its $10th$ percentile (i.e., outside deep recessions).

2.5 Simulation Evidence

Before proceeding, it is important to test the ability of the IVAR and the non-recursive identification scheme to estimate the effects of uncertainty shocks and capture any state-dependence in these responses. We therefore simulate $\{\mathbf{Y}_t\}_{t=1}^{S}$ from the DSGE model presented below and estimate the IVAR on this sample using a relatively high value of $S = 3,000$ to sidestep issues related to sampling uncertainty. The adopted identifying assumptions for uncertainty shocks on this simulated sample are similar to those presented above, except for two minor modifications. First, when working with historical data, we locate extreme observations for volatility as periods when spikes in the VXO (i.e., the conditional volatility of the stock market return R_t^m) coincide with spikes in the financial uncertainty proxy of Ludvigson et al. (2019), which is an estimated stochastic volatility process extracted from a rich panel of financial variables. This volatility proxy is not available in our simulated sample, and we therefore replace it by the stochastic volatility process in the DSGE model. This implies that extreme observations for volatility in our

[6] There are two reasons to focus on a single model instead of the entire identified set. First, our goal is to estimate a DSGE model by matching impulse responses and we therefore have to focus on a single set of responses from the IVAR. Second, the confidence bands for the GIRFs can be computed by a standard bootstrap algorithm when focusing on a single model. However, in our Online Appendix, we show that for *all* models belonging to the set $\mathcal{B}$, the response of real activity to an uncertainty shock is stronger in recessions than in expansions.

simulated sample are episodes when the conditional volatility of R^m and the stochastic volatility shocks both are high and exceed their 50th percentile across all unconstrained solutions in $\mathcal{B}$. Second, the DSGE model presented below does not include a gold price, and we are therefore unable to include the correlation restriction between the real gold price and uncertainty shocks in the simulation study.

Figure 3: Simulation Exercise for the IVAR: IRFs to an Uncertainty Shock
This figure shows the generalized impulse response functions (GIRFs) in the IVAR to a positive one-standard deviation shock to uncertainty in strong expansions (to the left) and deep recessions (to the right) on a simulated sample of 3,000 draws from the New Keynesian DSGE model using the estimates in column (1) of Table 4. The solid (dashed) lines report the median target impulse responses in strong expansions (deep recessions) when computed as suggested by Fry and Pagan (2011), while the identified sets in the IVAR are denoted by the shaded areas. The marked solid lines denote the true responses in the DSGE model. All responses are shown in percentage deviations, except for the policy rate where changes in percentage points are reported.

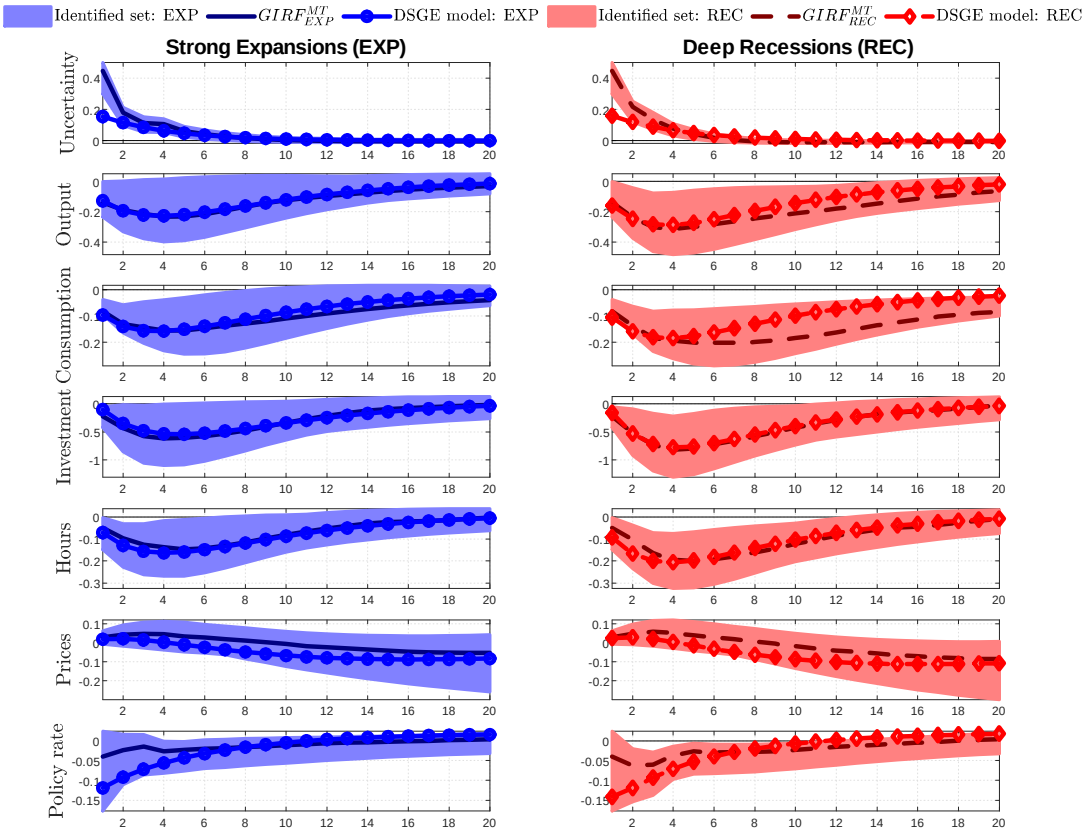

The results from this simulation exercise are summarized in Figure 3. Very encouragingly, we find that the identified set for uncertainty shocks in the IVAR (denoted by the shaded areas) nearly always contains the true responses in the DSGE model.[7] A careful

[7] The exception is for the responses in uncertainty (i.e. VXO), which exceed the true responses in the first couple of periods after the uncertainty shock. Unreported results show that this upward bias is closely

inspection of Figure 3 also shows that the IVAR is able to generate state-dependent effects in the responses, and that they match those in the DSGE model. This is especially the case for investment and hours, where we see large differences between recessions and expansions.[8]

We draw two conclusions from this simulation exercise. First, the non-recursive identifying scheme in the IVAR is sufficiently flexible to capture the responses of uncertainty shocks in our DSGE model. Second, any state-dependence in the responses to uncertainty shocks are well captured by the IVAR in (1). Thus, an important econometric implication of this simulation exercise is that the GIRFs from the IVAR can be used for a direct inference approach when estimating our DSGE model.

3 A New Keynesian Model

This section presents a New Keynesian DSGE model to explain why uncertainty shocks have larger effects in recessions than in expansions. Our starting point is the model by Basu and Bundick (2017) and its refinement in Basu and Bundick (2018). We extend this model along three dimensions. First, external consumption habits are included to capture a hump-shaded response in consumption to an uncertainty shock. Second, the flexible formulation of recursive preferences in Andreasen and Jørgensen (2020) is adopted to keep risk aversion at a low and plausible level. Finally, standard cost-push shocks are introduced to match the comovement between consumption and output across the business cycle. Given that the basic structure of this New Keynesian model is widely known, we only present its crucial parts and defer a full presentation with derivations to the Online Appendix.

3.1 Households

We consider an infinitely lived representative household with recursive preferences as in Epstein and Zin (1989) and Weil (1990). Using the formulation in Rudebusch and Swanson (2012), the value function V_t is given by

$$V_t = \begin{cases} u_t + \beta(\mathbb{E}_t\left[V_{t+1}^{1-\alpha}\right])^{\frac{1}{1-\alpha}} & \text{when } u_t > 0 \text{ for all } t \\ u_t - \beta(\mathbb{E}_t\left[(-V_{t+1})^{1-\alpha}\right])^{\frac{1}{1-\alpha}} & \text{when } u_t < 0 \text{ for all } t \end{cases}, \tag{3}$$

related to the adopted simulation procedure for the VXO which is $100\sqrt{4\max\left\{\mathbb{V}_t\left[R_{t+1}^m\right], 0.000026\right\}}$ as suggested by the codes related to Basu and Bundick (2018). By imposing this lower bound for the conditional variance of stock returns $\mathbb{V}_t\left[R_{t+1}^m\right]$, we get an upward bias in the IVAR residuals for $\log VXO_t$ and subsequently also an upward bias in the impulse response functions for $\log VXO_t$.

[8] See also the Online Appendix, where we also plot the median target responses.

where u_t is the utility function and $\mathbb{E}_t[\cdot]$ is the conditional expectation in period t. The parameter $\alpha \in \mathbb{R} \setminus \{1\}$ captures households' appetite for the resolution of uncertainty, implying preferences for early (late) resolution of uncertainty if $\alpha > 0$ ($\alpha < 0$) for $u_t > 0$, and vice versa when $u_t < 0$. Andreasen and Jørgensen (2020) further argue that the size of this timing attitude is proportional to α, meaning that numerically larger values of α imply stronger preferences for early (late) resolution of uncertainty.

The expression for households' utility at time t is

$$u_t \equiv a_t^{1-\sigma}\left(\frac{1}{1-\sigma}\left(\left(C_t - bC_{t-1}\right)^{\eta}\left(1-N_{t,}\right)^{1-\eta}\right)^{1-\sigma} + u_0\right), \tag{4}$$

which depends on habit-adjusted consumption $C_t - bC_{t-1}$ and leisure $1 - N_t$.[9] As in Basu and Bundick (2017), a_t is a preference shock that evolves according to the process $a_{t+1} = \rho_a a_t + \sigma_{a,t}\epsilon_{a,t+1}$ where $\epsilon_{a,t+1} \sim \mathcal{NID}(0,1)$. The process for stochastic volatility $\sigma_{a,t}$ is specified as $\sigma_{a,t+1} = (1-\rho_\sigma) + \rho_\sigma \sigma_{a,t} + \sigma_\sigma \epsilon_{\sigma,t+1}$, where the innovations in uncertainty $\epsilon_{\sigma,t+1} \sim \mathcal{NID}(0,1)$ and uncorrelated with $\epsilon_{a,t+1}$ at all leads and lags. The constant u_0 captures utility from government spending and goods produced and consumed within the household. As shown by Andreasen and Jørgensen (2020), the main reason for including u_0 is to separately control the level of the utility function and hence disentangle the timing attitude α from relative risk aversion (RRA), which otherwise are tightly linked in the standard formulation of recursive preferences in Epstein and Zin (1989) and Weil (1990). To see this, note that (3) and (4) imply

$$\text{RRA} = \frac{\eta}{1-b}\left[\sigma + \alpha(1-\sigma)\frac{\left(\left(C_{ss} - bC_{ss}\right)^{\eta}\left(1-N_{ss}\right)^{1-\eta}\right)^{1-\sigma}}{\left(\left(C_{ss} - bC_{ss}\right)^{\eta}\left(1-N_{ss}\right)^{1-\eta}\right)^{1-\sigma} + (1-\sigma)u_0}\right],$$

at the deterministic steady state (ss) when accounting for the endogenous labor supply (see Swanson (2018)). Hence, a high timing attitude α does not necessarily imply a high RRA, which is in contrast to the standard case with $u_0 = 0$ where $\text{RRA} = \frac{\eta}{1-b}(\sigma + \alpha(1-\sigma))$.

The household receives labor income W_t for each unit of labor N_t supplied to the intermediate firms. These firms are owned by the household that therefore holds their equity shares S_t, which have the price P_t^E and pay dividends D_t^E. The household also holds one-period real bonds with the gross return R_t^R as issued by the firms, and it holds nominal bonds issued by the government with the gross return R_t.

[9] Following Basu and Bundick (2018), we include $a_t^{1-\sigma}$ instead of a_t in (4) to avoid having an asymptote in the policy function at $\sigma = 1$, as noted by de Groot et al. (2018).

3.2 Firms

The final output Y_t is produced by a representative final good producer using the production function $Y_t = \left(\int_0^1 Y_t(i)^{(\theta_{\mu,t}-1)/\theta_{\mu,t}}\, di\right)^{\theta_{\mu,t}/(\theta_{\mu,t}-1)}$, where $\theta_{\mu,t}$ captures a time-varying substitution elasticity between the intermediate goods $Y_t(i)$. It is assumed that $\log(\theta_{\mu,t+1}/\theta_\mu) = \rho_{\theta_\mu}\log(\theta_{\mu,t}/\theta_\mu) + \sigma_{\theta_\mu}\epsilon_{\theta,t+1}$, where $\epsilon_{\theta,t+1} \sim \mathcal{NID}(0,1)$. Cost minimization implies that $Y_t(i) = \left[\frac{P_t(i)}{P_t}\right]^{-\theta_{\mu,t}} Y_t$, where $P_t \equiv \left(\int_0^1 P_t(i)^{1-\theta_{\mu,t}}\, di\right)^{\frac{1}{1-\theta_{\mu,t}}}$ denotes the aggregate price level and $P_t(i)$ is the price of the ith good.

Intermediate firms produce $Y_t(i)$ using the Cobb-Douglas production function with fixed costs, i.e., $Y_t(i) = (K_{t-1}(i)U_t(i))^{\alpha_p}(Z_tN_t(i))^{1-\alpha_p} - \Phi$, where $K_{t-1}(i)$ is the capital stock, $U_t(i)$ is the utilization rate, and Z_t captures productivity shocks as $\log Z_{t+1} = \rho_Z \log Z_t + \sigma_Z\epsilon_{Z,t+1}$ with $\epsilon_{Z,t+1} \sim \mathcal{NID}(0,1)$. The capital stock evolves as $K_t(i) = \left(1 - \delta(U_t(i)) - \frac{\phi_K}{2}\left(I_t(i)/K_{t-1}(i) - \delta\right)^2\right)K_t(i) + I_t(i)$, where ϕ_K introduces adjustment costs and $I_t(i)$ is investment. The depreciation costs are given by $\delta(U_t(i)) = \delta + \delta_1(U_t(i) - U_{ss}) + \frac{\delta_2}{2}(U_t(i) - U_{ss})^2$. Intermediate firms operate in a market with monopolistic competition and face quadratic adjustment costs as in Rotemberg (1982). The expression for real dividends therefore reads

$$\frac{D_t(i)}{P_t} = \left[\frac{P_t(i)}{P_t}\right]^{1-\theta_{\mu,t}} Y_t - \frac{W_t}{P_t}N_t(i) - I_t(i) - \frac{\phi_P}{2}\left(\frac{P_t(i)}{\Pi_{ss}P_{t-1}(i)} - 1\right)^2 Y_t$$

where W_t is the wage and Π_{ss} denotes inflation in the deterministic steady state. Each intermediate firm finances a fraction ν of its capital stock by issuing one-period riskless bonds, i.e., $B_t(i) = \nu K_{t-1}(i)$. As a result, the real dividend payments to equity holders are $D_t^E(i)/P_t = D_t(i)/P_t - \nu(K_{t-1}(i) - K_t(i)/R_t^R)$.

3.3 Monetary Policy and Stock Market Volatility

The central bank adjusts the nominal interest rate R_t to stabilize inflation around its target Π_{ss} and output growth according to the rule

$$\ln(R_t/R_{ss}) = \zeta_\Pi \log(\Pi_t/\Pi_{ss}) + \zeta_{\Delta Y}\log(Y_t/Y_{t-1}), \tag{5}$$

where $\Pi_t \equiv P_t/P_{t-1}$ denotes gross inflation.[10]

As in Basu and Bundick (2017), the gross stock market return is defined as $R_t^m = \left(D_t^E + P_t^E\right)/P_{t-1}^E$. The model-implied measure for stock market volatility is then given by $VXO_t = 100\sqrt{4 \times \mathbb{V}_t\left[R_{t+1}^m\right]}$, where $\mathbb{V}_t\left[R_{t+1}^m\right]$ is the quarterly conditional variance of R_{t+1}^m.

[10] Unreported results show no evidence of interest rate smoothing in (5) when using the estimator presented in Section 5.1.

3.4 Equilibrium

We focus on the symmetric equilibrium, where all intermediate firms choose the same price $P_t(i) = P_t$, employ the same amount of labor $N_t(i) = N_t$, and choose the same level of capital $K_t(i) = K_t$ and utilization rate $U_t(i) = U_t$. Consequently, all firms have the same cash flows and are financed with the same mix of bonds and equity. The markup of the price in relation to marginal cost is $\mu_t = 1/\Xi_t$, where Ξ_t denotes the marginal cost of producing one additional unit by the intermediate firm.

4 Model Solution

This section derives a third-order approximation to DSGE models around the risky steady state and study some of its implications. Section 4.1 describes a general class of DSGE models that includes the New Keynesian model presented above. The third-order Taylor approximation around the risky steady state is derived in Section 4.2, and we discuss a pruned version of this approximation in Section 4.3. The accuracy and execution time of various approximations are studied in Section 4.4.

4.1 General Model

We consider the class of models where the equilibrium conditions are given by

$$\mathbb{E}_t \left[\mathbf{f} \left(\mathbf{y}_{t+1}, \mathbf{y}_t, \mathbf{x}_{t+1}, \mathbf{x}_t \right) \right] = \mathbf{0}. \tag{6}$$

The states appear in $\mathbf{x}_t$ with dimension $n_x \times 1$, while the control variables of dimension $n_y \times 1$ are collected in $\mathbf{y}_t$, with $n \equiv n_x + n_y$. We also let $\mathbf{x}_t \equiv \begin{bmatrix} \mathbf{x}_{1,t}' & \mathbf{x}_{2,t}' \end{bmatrix}'$, where $\mathbf{x}_{1,t}$ refers to the endogenous states and $\mathbf{x}_{2,t}$ to the exogenous states, which evolve as

$$\mathbf{x}_{2,t+1} = \mathbf{h}_2 \left(\mathbf{x}_{2,t} \right) + \tilde{\boldsymbol{\eta}} \boldsymbol{\epsilon}_{t+1}, \tag{7}$$

where $\boldsymbol{\epsilon}_{t+1} \sim \mathcal{IID} \left(\mathbf{0}, \mathbf{I}_{n_\epsilon} \right)$, and n_ϵ is the number of elements in the vector of shocks $\boldsymbol{\epsilon}_{t+1}$.[11] The assumption that the innovations enter linearly in (7) is without loss of generality, because the state vector may be extended to account for nonlinearities between $\mathbf{x}_t$ and $\boldsymbol{\epsilon}_{t+1}$, as needed when including stochastic volatility in the exogenous states (see Andreasen (2012) for further details). The exact solution to this class of models is given by

$$\mathbf{y}_t = \mathbf{g} \left(\mathbf{x}_t \right) \tag{8}$$

[11] All eigenvalues of $\partial \mathbf{h}_2 \left(\mathbf{x}_{2,t} \right) / \partial \mathbf{x}_{2,t}$ must have modulus less than one, implying that trends may only be included if the model after re-scaling has an equivalent representation without trending variables. The procedure of re-scaling a DSGE model with trends is carefully described in King et al. (2002).

$$\mathbf{x}_{t+1} = \mathbf{h}\left(\mathbf{x}_t\right) + \boldsymbol{\eta}\boldsymbol{\epsilon}_{t+1} \tag{9}$$

where $\boldsymbol{\eta} \equiv \begin{bmatrix} \mathbf{0} & \tilde{\boldsymbol{\eta}}' \end{bmatrix}'$ has dimension $n_x \times n_\epsilon$. The functions $\mathbf{g}\left(\cdot\right)$ and $\mathbf{h}\left(\cdot\right)$ are generally unknown and must be approximated.

4.2 A Third-Order Approximation at the Risky Steady State

Let $\mathbf{x}_t = \bar{\mathbf{x}}$ denote the risky steady state. This long-term equilibrium point is characterized by the absence of structural shocks (i.e., $\boldsymbol{\epsilon}_{t+1} = \mathbf{0}$) but agents nevertheless respond to their probability distribution. This makes the risky steady state different from the widely used deterministic steady state, where agents do not respond to the probability distribution of the structural shocks.

The considered third-order approximation around $\bar{\mathbf{x}}$ is given by

$$\begin{aligned} \mathbf{y}_t &= \mathbf{g}\left(\bar{\mathbf{x}}\right) + \mathbf{g}_{\mathbf{x}}\left(\bar{\mathbf{x}}\right)\left(\mathbf{x}_t - \bar{\mathbf{x}}\right) + \tfrac{1}{2}\mathbf{g}_{\mathbf{xx}}\left(\bar{\mathbf{x}}\right)\left(\mathbf{x}_t - \bar{\mathbf{x}}\right)^{\otimes 2} + \tfrac{1}{6}\mathbf{g}_{\mathbf{xxx}}\left(\bar{\mathbf{x}}\right)\left(\mathbf{x}_t - \bar{\mathbf{x}}\right)^{\otimes 3} \\ \mathbf{x}_{t+1} &= \mathbf{h}\left(\bar{\mathbf{x}}\right) + \mathbf{h}_{\mathbf{x}}\left(\bar{\mathbf{x}}\right)\left(\mathbf{x}_t - \bar{\mathbf{x}}\right) + \tfrac{1}{2}\mathbf{h}_{\mathbf{xx}}\left(\bar{\mathbf{x}}\right)\left(\mathbf{x}_t - \bar{\mathbf{x}}\right)^{\otimes 2} + \tfrac{1}{6}\mathbf{h}_{\mathbf{xxx}}\left(\bar{\mathbf{x}}\right)\left(\mathbf{x}_t - \bar{\mathbf{x}}\right)^{\otimes 3} + \boldsymbol{\eta}\boldsymbol{\epsilon}_{t+1}, \end{aligned} \tag{10}$$

where $\left(\mathbf{x}_t - \bar{\mathbf{x}}\right)^{\otimes 2} \equiv \left(\mathbf{x}_t - \bar{\mathbf{x}}\right) \otimes \left(\mathbf{x}_t - \bar{\mathbf{x}}\right)$ and $\left(\mathbf{x}_t - \bar{\mathbf{x}}\right)^{\otimes 3} \equiv \left(\mathbf{x}_t - \bar{\mathbf{x}}\right)^{\otimes 2} \otimes \left(\mathbf{x}_t - \bar{\mathbf{x}}\right)$. The first-order derivative of $\mathbf{g}\left(\mathbf{x}_t\right)$ with respect to $\mathbf{x}_t$ is denoted $\mathbf{g}_{\mathbf{x}}\left(\bar{\mathbf{x}}\right)$ when evaluated at $\bar{\mathbf{x}}$. A similar notation is used for $\mathbf{h}\left(\mathbf{x}_t\right)$ and for higher-order derivatives.[12] The procedure we use to compute the required derivatives of $\mathbf{g}\left(\cdot\right)$ and $\mathbf{h}\left(\cdot\right)$ is similar to the one applied in Collard and Juillard (2001*a*) for a simple endowment model and in Collard and Juillard (2001*b*) for a DSGE model solved by a second-order approximation. Hence, we substitute (8) and (9) into (6) to get

$$\mathbb{E}_t\left[\mathbf{F}\left(\mathbf{x}_t, \boldsymbol{\epsilon}_{t+1}\right)\right] \equiv \mathbb{E}_t\left[\mathbf{f}\left(\mathbf{g}\left(\mathbf{h}\left(\mathbf{x}_t\right) + \boldsymbol{\eta}\boldsymbol{\epsilon}_{t+1}\right), \mathbf{g}\left(\mathbf{x}_t\right), \mathbf{h}\left(\mathbf{x}_t\right) + \boldsymbol{\eta}\boldsymbol{\epsilon}_{t+1}, \mathbf{x}_t\right)\right] = \mathbf{0}. \tag{11}$$

We then compute a third-order Taylor approximation of $\mathbf{F}\left(\mathbf{x}_t, \boldsymbol{\epsilon}_{t+1}\right)$ at $\mathbf{x}_t = \bar{\mathbf{x}}$ and $\boldsymbol{\epsilon}_{t+1} = \mathbf{0}$. Evaluating the expectations with respect to terms that involve $\boldsymbol{\epsilon}_{t+1}$ and using the method of undetermined coefficients, we obtain the following conditions (derived in our Online Appendix):

$$\left[\mathbf{F}\left(\bar{\mathbf{x}}, \mathbf{0}\right)\right]^i + \frac{1}{2}\left[\mathbf{F}_{\boldsymbol{\epsilon}\boldsymbol{\epsilon}}\left(\bar{\mathbf{x}}, \mathbf{0}\right)\right]^i_{\phi_1\phi_2}\left[\mathbb{V}\left[\boldsymbol{\epsilon}_{t+1}\right]\right]^{\phi_1}_{\phi_2} + \frac{1}{6}\left[\mathbf{F}_{\boldsymbol{\epsilon}\boldsymbol{\epsilon}\boldsymbol{\epsilon}}\left(\bar{\mathbf{x}}, \mathbf{0}\right)\right]^i_{\phi_1\phi_2\phi_3}\left[\mathbf{m}^3_{\epsilon}\right]^{\phi_1}_{\phi_2\phi_3} = 0 \tag{12}$$

$$\left[\mathbf{F}_{\mathbf{x}}\left(\bar{\mathbf{x}}, \mathbf{0}\right)\right]^i_{\alpha_1} + \frac{3}{6}\left[\mathbf{F}_{\boldsymbol{\epsilon}\boldsymbol{\epsilon}\mathbf{x}}\left(\bar{\mathbf{x}}, \mathbf{0}\right)\right]^i_{\phi_1\phi_2\alpha_3}\left[\mathbb{V}\left[\boldsymbol{\epsilon}_{t+1}\right]\right]^{\phi_1}_{\phi_2} = 0 \tag{13}$$

$$\left[\mathbf{F}_{\mathbf{xx}}\left(\bar{\mathbf{x}}, \mathbf{0}\right)\right]^i_{\alpha_1\alpha_2} = 0 \tag{14}$$

$$\left[\mathbf{F}_{\mathbf{xxx}}\left(\bar{\mathbf{x}}, \mathbf{0}\right)\right]^i_{\alpha_1\alpha_2\alpha_3} = 0, \tag{15}$$

[12] Note that $\bar{\mathbf{x}}$ is a fixed-point in $\mathbf{h}\left(\cdot\right)$, i.e. $\mathbf{h}\left(\bar{\mathbf{x}}\right) = \bar{\mathbf{x}}$, and that the ergodic mean $\mathbb{E}\left[\mathbf{x}_t\right]$ generally differs from the risky steady state $\bar{\mathbf{x}}$ because $\mathbb{E}\left[\mathbf{x}_{t+1} - \bar{\mathbf{x}}\right] = \mathbb{E}\left[\frac{1}{2}\mathbf{h}_{\mathbf{xx}}\left(\bar{\mathbf{x}}\right)\left(\mathbf{x}_t - \bar{\mathbf{x}}\right)^{\otimes 2} + \frac{1}{6}\mathbf{h}_{\mathbf{xxx}}\left(\bar{\mathbf{x}}\right)\left(\mathbf{x}_t - \bar{\mathbf{x}}\right)^{\otimes 3}\right] \neq 0$.

where the tensor notation is used with $i = \{1, 2, ..., n\}$, $\phi_1, \phi_2, \phi_3 = \{1, 2, ..., n_\epsilon\}$, and $\alpha_1, \alpha_2, \alpha_3 = \{1, 2, ..., n_x\}$. Also, $\mathbb{V}[\boldsymbol{\epsilon}_{t+1}]$ is the covariance matrix of $\boldsymbol{\epsilon}_{t+1}$ (which equals $\mathbf{I}_{n_\epsilon}$), and $\mathbf{m}_\epsilon^3$ with dimensions $n_\epsilon \times n_\epsilon \times n_\epsilon$ contains all third order moments of $\boldsymbol{\epsilon}_{t+1}$. The derivatives of $\mathbf{F}(\mathbf{x}_t, \boldsymbol{\epsilon}_{t+1})$ are denoted with subscripts and evaluated at the risky steady state, e.g., $\mathbf{F}_{\mathbf{x}}(\bar{\mathbf{x}}, \mathbf{0}) = \partial \mathbf{F}(\mathbf{x}_t, \boldsymbol{\epsilon}_{t+1}) / \partial \mathbf{x}_t'|_{\mathbf{x}_t = \bar{\mathbf{x}}, \boldsymbol{\epsilon}_{t+1} = \mathbf{0}}$.

To understand the implications of (12) to (15), let us first consider the case without uncertainty by letting $\mathbb{V}[\boldsymbol{\epsilon}_{t+1}] = \mathbf{0}$ and $\mathbf{m}^3(\boldsymbol{\epsilon}_{t+1}) = \mathbf{0}$ to obtain the certainty equivalence solution. The $n \times 1$ equations in (12) then simplifies to $[\mathbf{F}(\bar{\mathbf{x}}, \mathbf{0})]^i = 0$, implying that $\bar{\mathbf{x}} = \mathbf{x}_{ss}$ and $\bar{\mathbf{y}} = \mathbf{y}_{ss}$. We also have that (13) reduces to $[\mathbf{F}_{\mathbf{x}}(\mathbf{x}_{ss}, \mathbf{0})]^i_{\alpha_1} = 0$, which gives the well-known quadratic system for computing the first-order derivatives $\mathbf{g}_{\mathbf{x}}(\mathbf{x}_{ss})$ and $\mathbf{h}_{\mathbf{x}}(\mathbf{x}_{ss})$, as shown in Schmitt-Grohe and Uribe (2004). Moreover, (14) reduces to $[\mathbf{F}_{\mathbf{xx}}(\mathbf{x}_{ss}, \mathbf{0})]^i_{\alpha_1\alpha_2} = 0$ and (15) to $[\mathbf{F}_{\mathbf{xxx}}(\mathbf{x}_{ss}, \mathbf{0})]^i_{\alpha_1\alpha_2\alpha_3} = 0$, which are the linear systems exploited by the standard perturbation method to compute the second-order terms $\mathbf{g}_{\mathbf{xx}}(\mathbf{x}_{ss})$ and $\mathbf{h}_{\mathbf{xx}}(\mathbf{x}_{ss})$ and the third-order terms $\mathbf{g}_{\mathbf{xxx}}(\mathbf{x}_{ss})$ and $\mathbf{h}_{\mathbf{xxx}}(\mathbf{x}_{ss})$, respectively (see Schmitt-Grohe and Uribe (2004) and Andreasen (2012)). Thus, without uncertainty, the conditions in (12) to (15) are identical to those used by the standard perturbation method to obtain the certainty equivalent part of this approximation.

In the presence of uncertainty, condition (12) still determines $\bar{\mathbf{x}}$ and $\bar{\mathbf{y}}$, but in this case $\bar{\mathbf{x}} \neq \mathbf{x}_{ss}$ and $\bar{\mathbf{y}} \neq \mathbf{y}_{ss}$. Given $(\bar{\mathbf{x}}, \bar{\mathbf{y}})$, condition (13) allows us to determine the first-order derivatives of $\mathbf{g}(\cdot)$ and $\mathbf{h}(\cdot)$ by solving a quadratic system that includes the variance term $\frac{3}{6}[\mathbf{F}_{\boldsymbol{\epsilon}\boldsymbol{\epsilon}\mathbf{x}}(\bar{\mathbf{x}}, \mathbf{0})]^i_{\phi_1\phi_2\alpha_3}[\mathbb{V}[\boldsymbol{\epsilon}_{t+1}]]^{\phi_1}_{\phi_2}$. This adjustment has two important implications. First, it implies that the first-order derivatives $\mathbf{g}_{\mathbf{x}}(\bar{\mathbf{x}})$ and $\mathbf{h}_{\mathbf{x}}(\bar{\mathbf{x}})$ contain an uncertainty correction for variance risk. Second, the Blanchard-Kahn conditions for getting unique and stable first-order derivatives have to hold for a risk-adjusted version of the model. Hence, uncertainty may contribute to violate or satisfy the Blanchard-Kahn conditions, unlike in the standard perturbation method where these conditions are evaluated at the deterministic steady state. Importantly, the uncertainty correction $\frac{3}{6}[\mathbf{F}_{\boldsymbol{\epsilon}\boldsymbol{\epsilon}\mathbf{x}}(\bar{\mathbf{x}}, \mathbf{0})]^i_{\phi_1\phi_2\alpha_3}[\mathbb{V}[\boldsymbol{\epsilon}_{t+1}]]^{\phi_1}_{\phi_2}$ is of third order and therefore not present in the second-order approximation around the risky steady state as studied in Collard and Juillard (2001*b*).

The condition in (14) for the second-order terms $\mathbf{g}_{\mathbf{xx}}(\bar{\mathbf{x}})$ and $\mathbf{h}_{\mathbf{xx}}(\bar{\mathbf{x}})$ is similar to the one used in the standard perturbation method, except that all derivatives of $\mathbf{F}(\cdot)$, $\mathbf{g}(\cdot)$, and $\mathbf{h}(\cdot)$ are evaluated at the risky steady state. This implies that $\mathbf{g}_{\mathbf{xx}}(\bar{\mathbf{x}})$ and $\mathbf{h}_{\mathbf{xx}}(\bar{\mathbf{x}})$ contain a correction for uncertainty, which is essential for our analysis, because it enables us to obtain impulse response functions for uncertainty shocks that are state-dependent. Finally, the condition in (15) allows us to determine $\mathbf{g}_{\mathbf{xxx}}(\bar{\mathbf{x}})$ and $\mathbf{h}_{\mathbf{xxx}}(\bar{\mathbf{x}})$ by solving a linear system, where all derivatives of $\mathbf{F}(\cdot)$, $\mathbf{g}(\cdot)$, and $\mathbf{h}(\cdot)$ are evaluated at the risky steady state. As a result, $\mathbf{g}_{\mathbf{xxx}}(\bar{\mathbf{x}})$ and $\mathbf{h}_{\mathbf{xxx}}(\bar{\mathbf{x}})$ are also adjusted for uncertainty for the same reasons as mentioned for $\mathbf{g}_{\mathbf{xx}}(\bar{\mathbf{x}})$ and $\mathbf{h}_{\mathbf{xx}}(\bar{\mathbf{x}})$.[13] For the New Keynesian model we

[13] Very loosely, one can think of $\mathbf{g}_{\mathbf{x}}(\bar{\mathbf{x}}) \approx \mathbf{g}_{\mathbf{x}}(\mathbf{x}_{ss}) + 0.5\mathbf{g}_{\sigma\sigma\mathbf{x}}(\mathbf{x}_{ss})$ and $\mathbf{h}_{\mathbf{x}}(\bar{\mathbf{x}}) \approx \mathbf{h}_{\mathbf{x}}(\mathbf{x}_{ss}) + 0.5\mathbf{h}_{\sigma\sigma\mathbf{x}}(\mathbf{x}_{ss})$,

consider, nearly all of the uncertainty correction in the higher-order derivatives comes from the risk adjustment in $\mathbf{g}_{\mathbf{x}}(\bar{\mathbf{x}})$ and $\mathbf{h}_{\mathbf{x}}(\bar{\mathbf{x}})$, meaning that a third-order approximation is needed for our model to get visible state-dependence in the impulse response functions for an uncertainty shock.[14]

Unfortunately, the moment conditions in (12) to (15) do not imply a recursive structure for computing the required terms in (10). This is because $\mathbf{F}_{\boldsymbol{\epsilon\epsilon}}(\bar{\mathbf{x}}, \mathbf{0})$, $\mathbf{F}_{\boldsymbol{\epsilon\epsilon x}}(\bar{\mathbf{x}}, \mathbf{0})$, and $\mathbf{F}_{\boldsymbol{\epsilon\epsilon\epsilon}}(\bar{\mathbf{x}}, \mathbf{0})$ depend on $(\bar{\mathbf{x}}, \bar{\mathbf{y}})$ and the derivatives of $\mathbf{g}(\cdot)$ and $\mathbf{h}(\cdot)$. We therefore use an iterative procedure, where $\mathbf{F}_{\boldsymbol{\epsilon\epsilon}}(\bar{\mathbf{x}}, \mathbf{0})$, $\mathbf{F}_{\boldsymbol{\epsilon\epsilon x}}(\bar{\mathbf{x}}, \mathbf{0})$, and $\mathbf{F}_{\boldsymbol{\epsilon\epsilon\epsilon}}(\bar{\mathbf{x}}, \mathbf{0})$ are computed using derivatives of $\mathbf{g}(\cdot)$ and $\mathbf{h}(\cdot)$ from the standard perturbation method in the first iteration and afterwards from the previous iteration to recursively solve (12) to (15). Our Online Appendix summarizes this algorithm, which basically iterates on the solution routine for the standard perturbation approximation until convergence (typically with five iterations).[15]

4.3 A Pruned State-Space Representation

The system for a standard third-order perturbation approximation obviously reduces to the system in (10) when all derivatives of the **g**- and **h**-functions with respect to the perturbation parameter are equal to zero. This means that the pruning scheme introduced in Andreasen et al. (2018) can also be applied to (10) with all derivatives of the **g**- and **h**-functions with respect to $\mathbf{x}_t$ evaluated at $\bar{\mathbf{x}}$ instead of $\mathbf{x}_{ss}$. The Blanchard-Kahn condition related to (13) ensures that $\mathbf{h}_{\mathbf{x}}(\bar{\mathbf{x}})$ is stable and hence that this pruned approximation is stable. Thus, the closed-form solution for unconditional moments and GIRFs derived in Andreasen et al. (2018) can also be applied to our third order approximation at the risky steady state. This greatly facilitates its use in a formal estimation routine that matches unconditional first and second moments, impulse response functions, or a combination of the two, as considered below in Section 5.

---

where σ is the perturbation parameter as defined in Schmitt-Grohe and Uribe (2004). In the standard perturbation method, only $\mathbf{g}_{\mathbf{x}}(\mathbf{x}_{ss})$ and $\mathbf{h}_{\mathbf{x}}(\mathbf{x}_{ss})$ are used to compute the higher-order derivatives. In contrast, the procedure we use implies that $\mathbf{g}_{\mathbf{x}}(\mathbf{x}_{ss}) + 0.5\mathbf{g}_{\sigma\sigma\mathbf{x}}(\mathbf{x}_{ss})$ and $\mathbf{h}_{\mathbf{x}}(\mathbf{x}_{ss}) + 0.5\mathbf{h}_{\sigma\sigma\mathbf{x}}(\mathbf{x}_{ss})$ are used to compute the higher-order derivatives, which therefore include an adjustment for uncertainty.

[14] As shown in the Online Appendix, the expressions for $\mathbf{F}_{\boldsymbol{\epsilon\epsilon}}(\bar{\mathbf{x}}, \mathbf{0})$, $\mathbf{F}_{\boldsymbol{\epsilon\epsilon x}}(\bar{\mathbf{x}}, \mathbf{0})$, and $\mathbf{F}_{\boldsymbol{\epsilon\epsilon\epsilon}}(\bar{\mathbf{x}}, \mathbf{0})$ are identical to those provided for $\mathbf{F}_{\boldsymbol{\sigma\sigma}}$, $\mathbf{F}_{\boldsymbol{\sigma\sigma x}}$, and $\mathbf{F}_{\boldsymbol{\sigma\sigma\sigma}}$, respectively, in Schmitt-Grohe and Uribe (2004) and Andreasen (2012), when setting all derivatives of $\mathbf{g}(\cdot)$ and $\mathbf{h}(\cdot)$ with respect to the perturbation parameter σ equal to zero. The conditions in (12) to (15) are therefore easy to implement from existing results and computer packages on the standard perturbation method. In our case, we modify the highly efficient Matlab codes of Binning (2013).

[15] The proposed solution in (10) is, strictly speaking, not a perturbation approximation, because it does not perturb a known solution. Instead, it corresponds to a projection approximation that only exploits local properties of the model solution, and it is therefore best characterized as a local projection approximation.

4.4 Accuracy and Execution Time

We evaluate the accuracy of Taylor approximations around the deterministic and risky steady state by computing unit-free Euler-equation errors for the considered New Keynesian model along a simulated sample of $10,000$ observations for the states. The two estimated versions of the New Keynesian model presented below in Table 4 are considered for this exercise, where the states are simulated using a standard third-order perturbation approximation, i.e., by a Taylor approximation around the deterministic steady state.

Table 3: Accuracy and Execution Time

Panel $\mathcal{A}$ in this table reports the mean absolute unit-free Euler-equation errors (MAEs) and the root mean squared unit-free Euler-equation errors (RMSEs) in a second-, third-, and fourth-order Taylor approximation around the deterministic steady state, and in a second- and third-order Taylor approximation around the risky steady state. All model equations are included when computing the MAEs and the RMSEs, except for the link-equations related to lagged controls and the equations for the exogenous shocks, where the errors always are zero. The Euler-equations errors are reported in percent and computed using a simulated sample path of 10,000 observations for the states. For each estimated version of the model, the simulated sample path is computed using a third-order Taylor approximation around the deterministic steady state. Conditional expectations in the Euler-equations are evaluated by Gauss-Hermite quadratures using five points per shock, giving a total of $5^4 = 625$ points. The considered model parameters are those reported in Table 4. Panel $\mathcal{B}$ shows the execution time in seconds for obtaining the approximated model solutions and for simulating 10,000 observations using each of the considered approximations. The computations are done on a standard laptop with an Intel(R) Core(TM) i7-7600 CPU processor with 2.80GHz.

		Taylor approximations at deterministic steady state			Taylor approximations at risky steady state	
		2nd	3rd	4th	2nd	3rd
Panel $\mathcal{A}$: Accuracy (in pct.)						
Benchmark	MAEs	1.19	1.10	0.65	1.06	0.79
	RMSEs	3.26	3.03	2.27	3.10	2.44
Standard EZ	MAEs	1.41	1.22	0.79	1.16	0.87
	RMSEs	3.98	3.44	5.61	3.45	3.44
Panel $\mathcal{B}$: Execution time (in sec.)						
Benchmark	Model solution	0.03	0.60	12.0	0.45	3.50
	Simulation of of 10,000 observations	0.13	1.04	22.4	0.13	1.04

For the benchmark model, panel $\mathcal{A}$ in Table 3 shows that the standard perturbation method performs fairly well, as the mean absolute Euler errors (MAEs) across all endogenous equations in the model are only 1.19% at second order, 1.10% at third order, and 0.65% at fourth order. We find a similar monotone improvement in accuracy by increasing the approximation order when computing the root mean squared Euler-equation errors (RMSEs), that penalize large errors more heavily than the MAEs. For approximations around the risky steady state, the second-order approximation of Collard and Juillard (2001*b*) provides a small improvement when compared to the standard perturbation method at second order, as the MAEs falls from 1.19% to 1.06% and the RMSEs

from 3.26% to 3.10%. We see more notable reductions in the Euler errors by using the proposed third-order approximation around the risky steady state, as the MAEs falls from 1.10% to 0.79% and the RMSEs from 3.03% to 2.44% when compared to a third-order approximation around $\mathbf{x}_{ss}$. Thus, the accuracy of our approximation clearly outperforms the standard perturbation method at third order and is close to providing the same level of accuracy as the fourth-order Taylor approximation around $\mathbf{x}_{ss}$ with a MAE of 0.65 and a RMSE of 2.27.

Table 3 shows that we broadly find the same results for the estimated version of the New Keynesian model with standard Epstein-Zin preferences, i.e., $u_0 = 0$. The only exception is that the RMSEs for the fourth-order Taylor approximation around $\mathbf{x}_{ss}$ is 5.61% and hence higher than both third-order approximations with RMSEs of 3.44%.

The execution time for the various approximations are provided in panel $\mathcal{B}$ of Table 3. The standard third-order perturbation approximation is obtained in just 0.60 seconds, while it takes 12 seconds to compute a fourth-order approximation using the codes of Levintal (2017). The required time for computing our third-order approximation around the risky steady state depends mainly on the number of iterations needed to obtain convergence, but the execution time is typically around 4 seconds. Thus, we get an approximated model solution with state-dependent impulse response functions following an uncertainty shock that is about three times faster than the existing alternative of using a fourth-order approximation. In addition, it is also more costly to use a fourth-order than a third-order approximation when simulating the model. This is illustrated at the bottom of Table 3, where it takes one second to simulate $10,000$ observations from a third-order approximation but about 22 seconds when using a fourth-order approximation.

To summarize, the proposed third-order Taylor approximation around the risky steady state delivers a high level of accuracy that is comparable to a fourth-order perturbation approximation but is computationally much more efficient than this fourth order alternative. This is particularly convenient when it comes to estimating DSGE models like ours, where uncertainty shocks are allowed to have state-dependent effects.[16]

5 Empirical Results for the New Keynesian Model

This section presents our empirical findings for the New Keynesian model. We introduce the adopted estimation methodology in Section 5.1, and discuss the estimated parameters in Section 5.2 and the model fit in Section 5.3.

[16] de Groot (2016) highlights another shortcoming of the third-order Taylor approximation at the deterministic steady state, as none of its terms account for the conditional standard deviation of volatility shocks, i.e. σ_σ. Unreported results show that our third-order Taylor approximation around the risky steady state corrects for σ_σ and hence also addresses this limitation of the standard solution method.

5.1 Estimation Methodology

To describe our estimation approach, let the vector $\boldsymbol{\gamma}$ contain the structural parameters of the New Keynesian model. As in Basu and Bundick (2017), we estimate $\boldsymbol{\gamma}$ using two sets of moments. The first set includes the MT responses from the IVAR for the first 20 periods following an uncertainty shock in expansions $\widehat{\boldsymbol{\psi}}_{EXP}$ and in recessions $\widehat{\boldsymbol{\psi}}_{REC}$ as presented in Section 2. The second source of information is a vector of unconditional sample moments $\widehat{\mathbf{m}}_T$, which ensures that the model also matches stylized unconditional properties of the US economy in addition to the conditional moments following an uncertainty shock. These unconditional moments are constructed using the same data as applied to estimate the IVAR. That is, we use inflation, the shadow rate of Wu and Xia (2016), output, investment, consumption, and hours (with the four latter series detrended as in Hamilton (2018)). The included moments are the mean of inflation and the policy rate, as well as the covariances and auto-covariances related to the standard deviations and correlations listed in Table 5. Hence, the adopted estimator is given by

$$\begin{aligned}\hat{\boldsymbol{\gamma}} = \underset{\boldsymbol{\gamma}\in\boldsymbol{\Gamma}}{\arg\min} \quad & \left(\widehat{\boldsymbol{\psi}}_{EXP} - \boldsymbol{\psi}_{EXP}(\boldsymbol{\gamma})\right)' \mathbf{V}_{EXP}^{-1} \left(\widehat{\boldsymbol{\psi}}_{EXP} - \boldsymbol{\psi}_{EXP}(\boldsymbol{\gamma})\right) + \\ & \left(\widehat{\boldsymbol{\psi}}_{REC} - \boldsymbol{\psi}_{REC}(\boldsymbol{\gamma})\right)' \mathbf{V}_{REC}^{-1} \left(\widehat{\boldsymbol{\psi}}_{REC} - \boldsymbol{\psi}_{REC}(\boldsymbol{\gamma})\right) + \\ & \Lambda \left(\widehat{\mathbf{m}}_T - \mathbf{m}(\boldsymbol{\gamma})\right)' \mathbf{W}^{-1} \left(\widehat{\mathbf{m}}_T - \mathbf{m}(\boldsymbol{\gamma})\right),\end{aligned} \tag{16}$$

where $\mathbf{V}_{EXP}$,$\mathbf{V}_{REC}$, and $\mathbf{W}$ are diagonal matrices containing bootstrapped standard errors for the related moments and $\boldsymbol{\Gamma}$ denotes the feasible domain of $\boldsymbol{\gamma}$. The moments in the New Keynesian model are denoted by $\boldsymbol{\psi}_{EXP}(\boldsymbol{\gamma})$, $\boldsymbol{\psi}_{REC}(\boldsymbol{\gamma})$, and $\mathbf{m}(\boldsymbol{\gamma})$, which we compute using the third-order pruned approximation around the risky steady state. The impulse responses to an uncertainty shock are here obtained using a procedure similar to the one applied in the IVAR. That is, for each $\boldsymbol{\gamma}$, we simulate $10,000$ observations for output in the New Keynesian model to find the set of states where output is below its 10% percentile (denoted $\mathbf{X}^{REC}$) and above its 90% percentile (denoted $\mathbf{X}^{EXP}$). The impulse response functions are then computed as the average of the GIRFs across these selected states, i.e., $\boldsymbol{\psi}_m(\boldsymbol{\gamma}, h) = \frac{1}{250}\sum_{i=1}^{250} GIRF_{\mathbf{Y}}(h, \delta_{unc}, \mathbf{x}^{(i)})$ for $\mathbf{x}^{(i)} \in \mathbf{X}^m$, where $\boldsymbol{\psi}_m(\boldsymbol{\gamma}) \equiv \{\boldsymbol{\psi}_m(\boldsymbol{\gamma}, h)\}_{h=1}^{20}$ and $m = \{EXP, REC\}$ using 250 selected states. The expression for $GIRF_{\mathbf{Y}}(h, \delta_{unc}, \mathbf{x}^{(i)})$ is here evaluated in closed form using the observation in Section 4.3, which greatly reduces the computational costs in relation to the estimation.[17] Finally, we set Λ to ensure that the model implies a reasonable fit to the unconditional moments, and hence replicates both the impulse responses from the IVAR and the selected unconditional macro moments.

[17] Given that a simulated sample is needed to find the two sets $\mathbf{X}^{rec}$ and $\mathbf{X}^{exp}$, we settle by only computing unconditional means in $\mathbf{m}(\boldsymbol{\gamma})$ in closed form, while all unconditional second moments in $\mathbf{m}(\boldsymbol{\gamma})$ are obtained from the simulated sample to avoid the more computational evolved expression for these moments provided in Andreasen et al. (2018).

While most of the structural parameters in the model are estimated, we calibrate a few parameters that would be hard to pin down by our estimation procedure. Following Basu and Bundick (2017), we calibrate $\nu = 0.9$ for firm leverage, $\alpha_p = 1/3$ in the production function, $\delta = 0.025$ for steady state capital depreciations, $\delta_2 = 0.0003$ in the function for depreciation costs (with $\delta_1 = 1/\beta - 1 + \delta$), and the fixed cost Φ to remove pure profit for intermediate firms using the procedure in Basu and Bundick (2017). For households, the values of N_{ss} and η are set to match a steady state Frisch labour supply of two.

5.2 Estimated Structural Parameters

The estimation results for our preferred version of the model are reported in the first column of Table 4, where RRA is constrained to a plausible level of ten. We find a standard value for the subjective discount factor ($\beta = 0.994$), and evidence in favor of habit formation in consumption ($b = 0.26$). The preference parameter σ is somewhat high at 39.06, but this reflects the low calibrated value of $\eta = 0.017$, and we therefore find a fairly standard exponent for consumption of $\eta\,(1-\sigma) = -0.64$ in (4). These estimates imply that $V_t < 0$, meaning that negative values of α reflect preferences for early resolution of risk. We find $\alpha = -138$, which is very similar to the estimate reported in Andreasen and Jørgensen (2020) when RRA = 10. Our estimate of α is also extremely precise, with a bootstrapped standard error of 3.89. To aid the interpretation of the estimated price adjustment parameter $\phi_P = 163$, Table 4 reports the corresponding Calvo parameter ξ_{Calvo} that implies the same slope of the aggregate supply relation as ϕ_P. We find $\xi_{Calvo} = 0.84$, which corresponds to an average price duration of about 6 quarters. The substitution elasticity θ_μ between intermediate goods is 6.45, which gives an average price markup of about 18%. Finally, the central bank assigns more weight to stabilizing inflation than output growth with $\zeta_\Pi = 1.04$ and $\zeta_{\Delta Y} = 0.39$.

Table 4: Estimated Structural Parameters

This table reports the estimated structural parameters in the New Keynesian model using (16) with $\Lambda = 10^5$, where bootstrapped standard errors are shown in parenthesis. These standard errors are obtained by simulated 196 samples of the same length as in the data from the IVAR model by drawing with replacement from the estimated residuals $\hat{\boldsymbol{\eta}}_t$, From these samples, the required sample moments for the estimator in (16) are generated, where the median target impulse responses, i.e. $\boldsymbol{B_{MT}}$, are used to identify uncertainty shocks. The results in column (1) are for the benchmark model where RRA = 10, which implies $u_0 = -1.01$. The results in column (2) are for the standard formulation of recursive preferences with $u_0 = 0$, where the estimates imply an RRA of 124. The estimates of ϕ_P are reported as the corresponding Calvo parameter ξ_{Calvo}, i.e. the probability of not adjusting prices, that gives the same slope of the aggregate supply relation.

Description		(1) Benchmark model	(2) Standard specification of recursive preferences ($u_0 = 0$)
β	Subjective discount factor	0.994 (0.002)	0.994 (0.002)
b	Habit formation	0.26 (0.04)	0.27 (0.04)
σ	Preference parameter	39.06 (0.30)	38.93 (0.29)
α	Timing attitude	−137.75 (3.08)	−144.37 (3.58)
ϕ_K	Investment adjustment costs	5.50 (0.90)	5.46 (0.90)
ξ_{Calvo}	Price stickiness	0.84 (0.06)	0.84 (0.05)
θ_μ	Substitution elasticity of goods	6.45 (1.59)	6.27 (1.63)
ζ_Π	Weight on inflation gap	1.04 (0.02)	1.04 (0.02)
$\zeta_{\Delta Y}$	Weight on output growth	0.39 (0.05)	0.39 (0.05)
Π_{ss}	Steady state inflation rate	1.015 (0.001)	1.015 (0.001)
Stochastic processes			
ρ_σ	Persistence of uncertainty shock	0.69 (0.08)	0.69 (0.08)
σ_σ	Volatility of uncertainty shock	1.04 (0.03)	1.05 (0.006)
ρ_a	Persistence of demand shock	0.96 (0.01)	0.96 (0.01)
σ_a	Volatility of demand shock $\times 10^3$	0.20 (0.04)	0.22 (0.04)
ρ_z	Persistence of technology shock	0.63 (0.06)	0.62 (0.08)
σ_z	Volatility of technology shock	0.005 (0.0006)	0.006 (0.0009)
ρ_{θ_μ}	Persistent of markup shock	0.68 (0.06)	0.66 (0.06)
σ_{θ_μ}	Volatility of markup shock	0.20 (0.007)	0.20 (0.006)

The second column in Table 4 shows the corresponding estimates when applying the standard formulation of recursive preferences with $u_0 = 0$. We find that the estimates are very similar (but not identical) to those reported for our preferred specification.

The key difference relates to RRA, which is 124 when $u_0 = 0$ and hence comparable to other estimates in the macro literature as in Binsbergen et al. (2012) and Rudebusch and Swanson (2012) but much larger than implied by micro evidence (see, for instance, Barsky et al. (1997)).

5.3 Model Fit

Figure 4 shows the ability of the New Keynesian model to reproduce the median target responses in the IVAR following an uncertainty shock of the same size in recessions and expansions. We find that the model successfully matches the drop in output, consumption, and the substantially larger reduction in investment, which is more severe in recessions than in expansions. This ability of the model to generate state-dependent effects of an uncertainty shock is seen clearly from Figure 5, which compares the responses in the New Keynesian model across expansions and recessions. The model produces also a larger contraction of hours in recessions than in expansions, though it does not quantitatively replicate the contraction estimated with the IVAR.[18] The effects on the price level are well matched in recessions, whereas the responses in expansions are at the lower end of the 90% confidence band. The negative response in the policy rate on impact is perfectly captured by the model, but it generally predicts a less accommodating path for the policy rate following uncertainty shocks than implied by the IVAR.

[18] It is well known that without modeling labor market frictions, the response of hours in this type of model tends to be weaker than in the data. See Basu and Bundick (2017) and Fernández-Villaverde and Guerron-Quintana (2020) for discussions on this point.

Figure 4: New Keynesian Model: IRFs to an Uncertainty Shock

This figure shows the impulse response functions following a positive one-standard deviation shock to uncertainty in the IVAR at the median target responses and their 90 percentage confidence bands. The corresponding responses in the the New Keynesian model are computed for $\epsilon_{\sigma,t} = 1$ using the estimates in column (1) of Table 4. The responses are shown for strong expansions (charts to the left) and deep recessions (charts to the right). All responses are shown in percentage deviations, except for the policy rate where changes in percentage points are reported.

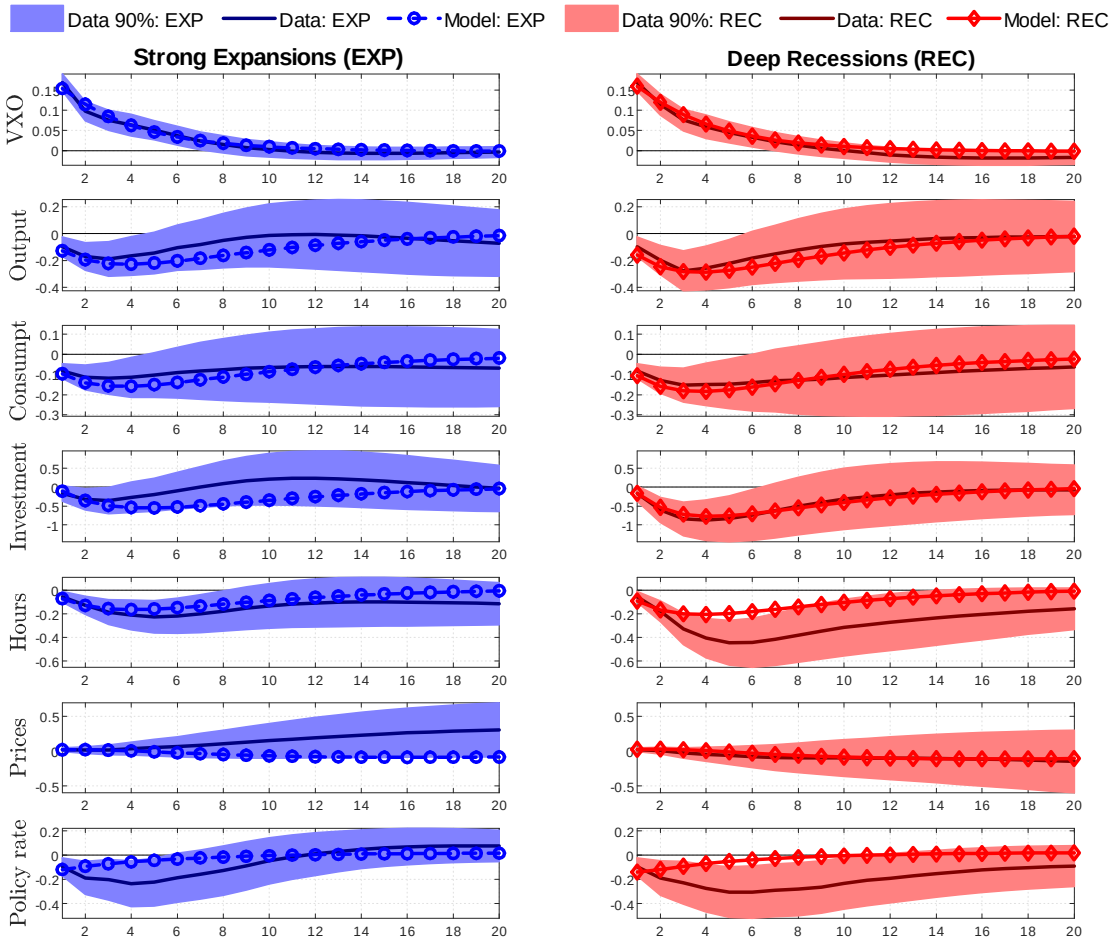

Table 5 reports the means and a scaled version of the second moments that also enter in the estimation. We find that the model closely matches the average level of inflation and the policy rate, while the mean of detrended output, consumption, investment and hours are (by construction) zero and therefore not included. The model is also successful in matching all standard deviations and autocorrelations, and it also captures the cross-correlations of consumption, investment, hours, inflation, and the policy rate with respect to detrended output.

Accordingly, this model goes a long way in reproducing the different impulse responses

Figure 5: New Keynesian Model: A State-Dependent Uncertainty Shock
This figure shows the impulse response functions following a positive one-standard deviation uncertainty shock (i.e. $\epsilon_{\sigma,t} = 1$) in the New Keynesian model using the estimates in column (1) of Table 4. The responses are shown for strong expansions and deep recessions. All responses are shown in percentage deviations, except for the policy rate where changes in percentage points are reported.

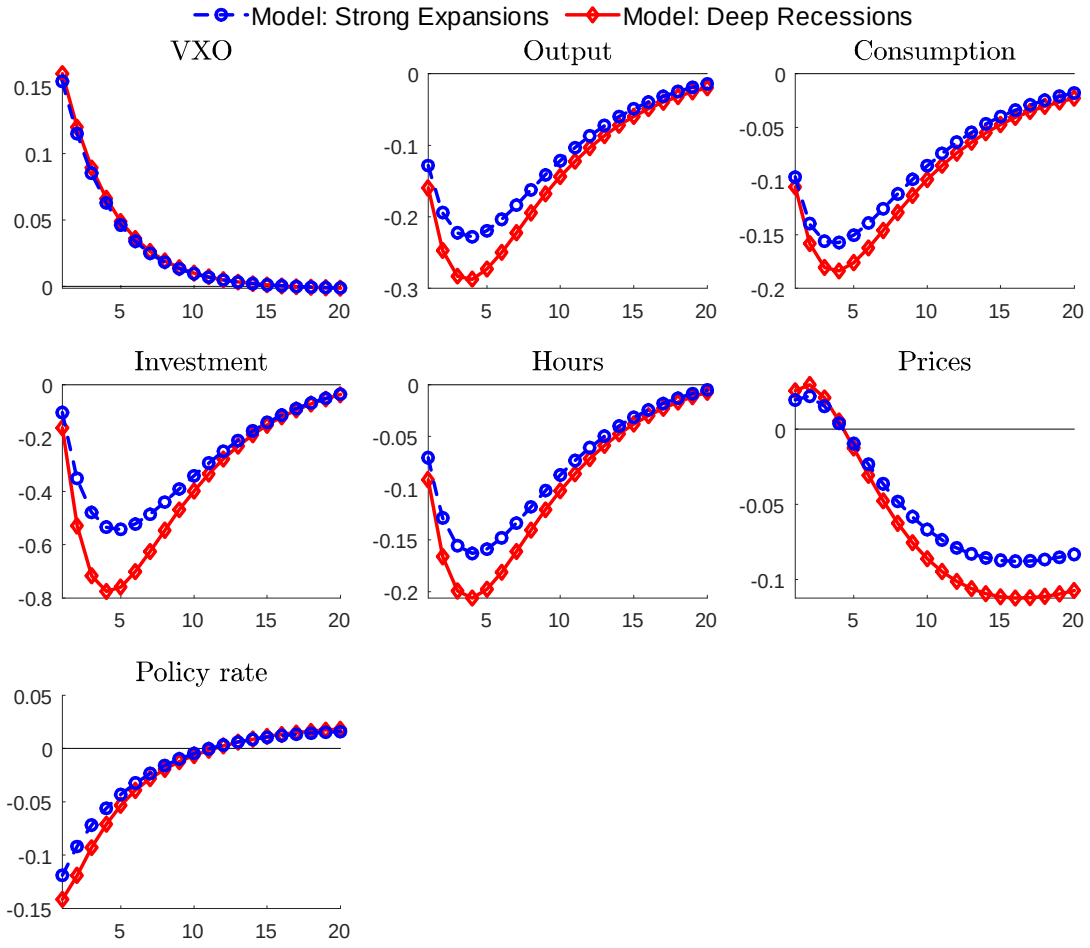

of real activity to an uncertainty shock in expansions and recessions, while providing a fairly accurate description of a variety of other macroeconomic moments. Crucially, the differences in these impulse responses between the two states of the business cycle are not explained by changes in the structural parameters or by larger uncertainty shocks in recessions than in expansions. Instead, these asymmetric responses are due to different initial conditions, as captured by the states $\mathbf{x}_t$, which through the model's endogenous propagation mechanisms make an uncertainty shock more severe in recessions than in expansions.

Table 5: New Keynesian Model: Fit to Unconditional Moments

This table reports the means along with the standard deviations and correlations that are related to the covariances and auto-covariances included in the estimator in (16). The data moments are computed using quarterly US data from 1962Q3 to 2017Q4, while the corresponding model-implied moments are computed in closed form for the means and using a simulated sample of $10,000$ observations for the second moments. Moments for output, consumption, investment, and hours are in deviation from steady state, as indicated by the "hat" notation, while the moments for inflation and the policy rate are annualized. The detrending of the moments in US data are done using the procedure in Hamilton (2018).

Moments	(1) Data	(2) Benchmark Model	(3) Standard specification of recursive preferences ($u_0 = 0$)
Means			
$\log \Pi_t$	0.034	0.034	0.033
$\log R_t$	0.051	0.055	0.056
Standard deviations			
$\hat{Y}_t$	0.034	0.036	0.036
$\hat{C}_t$	0.022	0.022	0.022
$\hat{I}_t$	0.101	0.098	0.099
$\hat{N}_t$	0.032	0.030	0.030
$\log \Pi_t$	0.022	0.025	0.026
$\log R_t$	0.041	0.025	0.026
Cross-correlations			
$corr(\hat{Y}_t, \hat{C}_t)$	0.86	0.68	0.65
$corr(\hat{Y}_t, \hat{I}_t)$	0.86	0.93	0.93
$corr(\hat{Y}_t, \hat{N}_t)$	0.90	0.96	0.96
$corr(\hat{Y}_t, \log \Pi_t)$	-0.38	-0.04	-0.05
$corr(\hat{Y}_t, \log R_t)$	-0.04	0.03	0.02
Auto-correlations			
$corr(\hat{Y}_t, \hat{Y}_{t-1})$	0.92	0.97	0.97
$corr(\hat{C}_t, \hat{C}_{t-1})$	0.90	0.97	0.96
$corr(\hat{I}_t, \hat{I}_{t-1})$	0.91	0.97	0.97
$corr(\hat{N}_t, \hat{N}_{t-1})$	0.91	0.96	0.96
$corr(\log \Pi_t, \log \Pi_{t-1})$	0.99	0.92	0.92
$corr(\log R_t, \log R_{t-1})$	0.97	0.96	0.96

6 Inspecting the Mechanisms

This section identifies the mechanisms in the New Keynesian model that generate larger effects of an uncertainty shock in recessions than in expansions. We first show in Section 6.1 that the state-dependent effects of an uncertainty shock are primarily generated by the upward nominal pricing-bias channel. The economic interpretation of this channel is

presented in Section 6.2, while Section 6.3 provides some external validation that supports the importance of this channel.

6.1 Channels for an Uncertainty Shock

As emphasized by Bianchi et al. (2019), each of the intertemporal Euler-equations in the model reflects expectations to uncertain realizations of state and control variables in the future and hence introduce different channels for an uncertainty shock to affect the economy. This implies that our model has the following channels for uncertainty shocks: i) the precautionary savings channel as captured by the consumption Euler-equation; ii) the nominal upward pricing bias channel as captured by the New Keynesian Phillips curve (NKPC) related to firms' optimality condition for the nominal price; iii) the inflation risk premium channel related to the Fisherian equation; and iv) the investment adjustment channel, that arises due to investment adjustment costs.[19]

We evaluate the relative importance of each channel by solving the model as described in Section 4, except that each Euler-equation is linearized one at the time to eliminate its implied channel for uncertainty shocks. For each of these modified solutions, we calculate the differences in the impulse responses between recessions and expansions, and compare them to the baseline case where all channels are active. Our findings are summarized in Figure 6. The results show that omitting the nominal pricing bias channel (the green line with stars) removes nearly all of the asymmetry in the responses between recessions and expansions, whereas none of the other channels have similar profound effects. This shows that the upward nominal pricing bias channel is the crucial channel to generate larger responses of output, consumption, investment, and hours to uncertainty shocks in recessions than in expansions.[20]

[19] The Euler-equation for stock returns may also imply an equity risk premium channel for uncertainty shocks. However, this channel is not present in our New Keynesian model because it omits feedback effects from the stock market to the real economy.

[20] In the Online Appendix we draw the same conclusion by considering the reverse exercise, where only the upward nominal pricing bias channel is active in the model. The Online Appendix also shows that the upward nominal pricing bias channel does not affect the overall magnitude of the impulse responses to an uncertainty shock but only the state-dependence of these responses.

6.2 A State-Dependent Upward Nominal Pricing Bias Channel

This upward nominal pricing bias channel arises because firms' profit function is asymmetric around the optimum in absence of uncertainty.[21] Hence, in the presence of uncertainty and sticky prices, it is beneficial for firms to set a relatively high nominal price. That is, firms respond to higher uncertainty by biasing their prices upwards. Our results show that firms bias their prices upward relatively more in recessions than in expansions and hence display a *state-dependent upward nominal pricing bias*. This effect is also evident from Figure 5, as prices in the baseline responses increase by more in recessions than in expansions following the first quarters after the uncertainty shock, whereas this difference disappears in Figure 6 when omitting the upward nominal pricing bias channel. To understand the state-dependent nature of this pricing bias, we first study the firm's pricing problem in a stylized two-period partial equilibrium setting, where the various effects are very transparent. The following subsection then shows that these insights carry over to the full general equilibrium model studied above.

6.2.1 A Two-Period Setting

Consider the following setting for the ith firm, which generalizes the static example in Fernández-Villaverde et al. (2015) and Born and Pfeifer (2020) to two periods and with quadratic price adjustment costs. The firm lives for two periods, and is initially at the deterministic steady state where $\Pi_{ss} = 1$ and $P_{ss} = 1$. No shocks affect real quantities, meaning that marginal costs $MC_t(i)$ and aggregate output Y_t are constant at $(\theta_\mu - 1)/\theta_\mu$ and 1, respectively. The objective of the firm is to set the current price $P_t(i)$ and the future price $P_{t+1}(i)$ when accounting for uncertainty about the aggregate price level in the next period, i.e., P_{t+1}, whereas the current price level is known at $P_t = 1$. The expression for real profit is otherwise identical to the one provided in the full model, except that future profits are discounted by β. Hence, the firm solves the problem

$$\underset{P_t(i),P_{t+1}(i)}{Max} \quad \sum_{j=\{0,1\}} \mathbb{E}_t \beta^j \left[\left(\frac{P_{t+j}(i)}{P_{t+j}} - \frac{\theta_\mu - 1}{\theta_\mu} \right) \left(\frac{P_{t+j}(i)}{P_{t+j}} \right)^{-\theta_\mu} - \frac{\phi_P}{2} \left(\frac{P_{t+j}(i)}{P_{t-1+j}(i)} - 1 \right)^2 \right]. \tag{17}$$

Suppose that the firm expects an aggregate price level in period $t+1$ of either $P_{t+1} = P_t + \sigma$ or $P_{t+1} = P_t - \sigma$ with equal probability. Without price adjustment costs ($\phi_P = 0$), it is easy to see that (17) reduces to two static optimization problems, where the current optimal price is $P_t(i) = 1$ (because P_t is known), and the optimal price in the next period $P_{t+1}(i)$ displays the familiar upward pricing bias due to uncertainty about P_{t+1} (see Fernández-Villaverde et al. (2015) and Born and Pfeifer (2020)). To illustrate the

[21] As clarified by Fernández-Villaverde et al. (2015) and Born and Pfeifer (2020), the asymmetry of the profit function is due to the combination of the isoelastic Dixit-Stiglitz demand function and the assumption that demand always has to be satisfied.

Figure 6: New Keynesian Model: Transmission Channels for an Uncertainty Shock

For a postive one-standard deviation uncertainty shock, this figure shows the difference in the responses between recessions and expansions. The baseline case is when all channels for uncertainty shocks are present in the model. A given channel is removed from this baseline by solving the model using a third-order approximation at the risky steady state with the modification that the Euler-equation for a particular channel is only linearized. All responses are computed using the estimates in column (1) of Table 4 for the New Keynesian model.

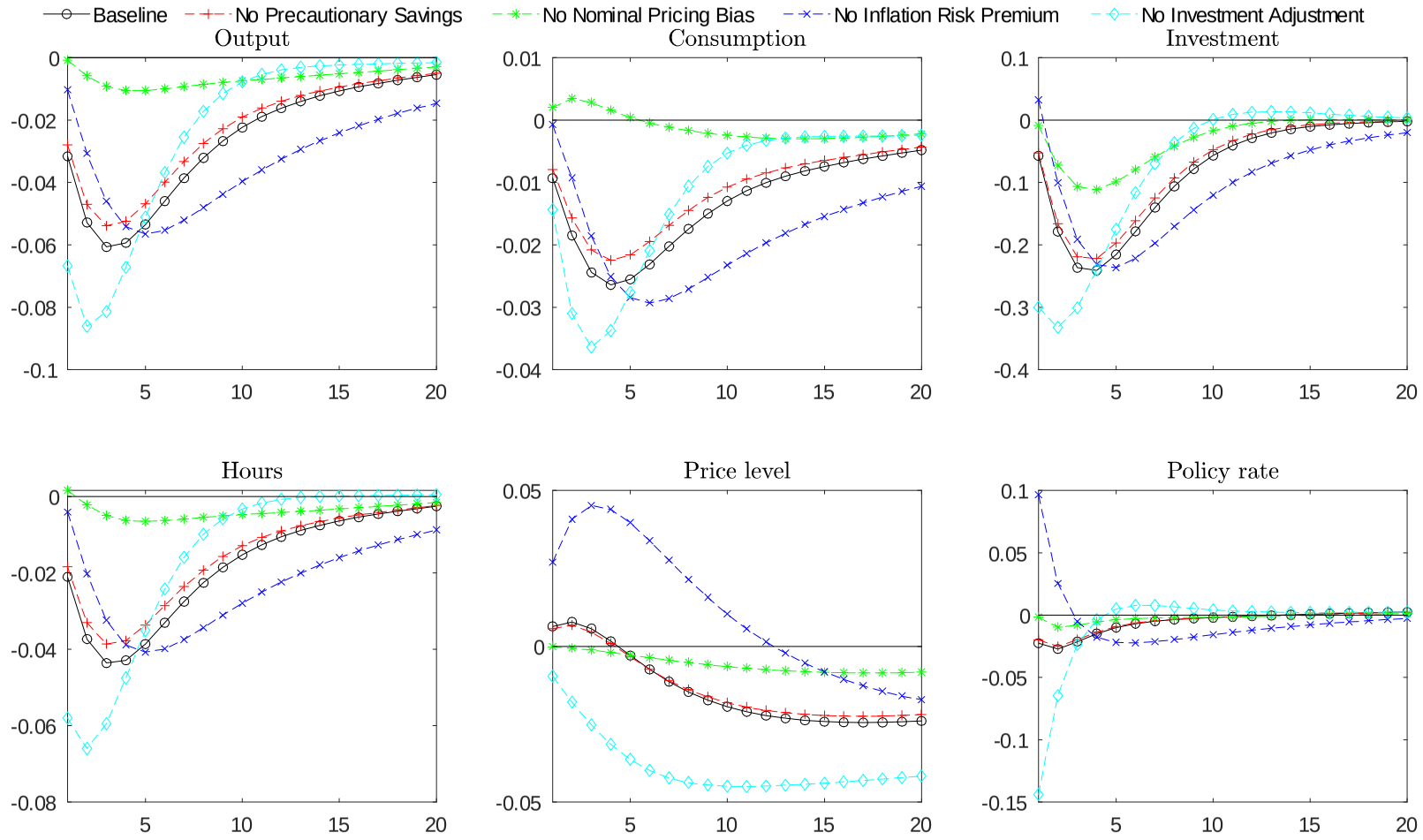

effects of accounting for price stickiness, we let $\theta_\mu = 6$, $\phi_P = 163$, and $\beta = 0.994$ as implied by our estimates in Table 4. The first chart in Figure 7 shows the profit function for different values of the current price $P_t(i)$ *around the optimum of* $P_{t+1}(i)$. The novel observation is that this profit function is asymmetric around one as $\phi_P > 0$, despite the aggregate price level P_t is known. In contrast, without price stickiness $\phi_P = 0$, the profit function is perfectly symmetric around one with a known price level, as shown in the Online Appendix. The second chart in Figure 7 plots the entire profit function and reveals that both $P_t(i)$ and $P_{t+1}(i)$ display upwards pricing biases. Thus, although there is no uncertainty about the current price level P_t, the presence of price stickiness makes it optimal for the firm to bias its current price upwards to smooth out its price adjustment costs. In other words, uncertainty about the aggregate price level in the next period is sufficient to generate an upward pricing bias in the current price $P_t(i)$. This is an important observation because it corresponds to the situation in the full general equilibrium model, as firms realize that uncertainty will be higher in the next period but already in the current period decide to bias their prices upwards.

Figure 7: The Firm's Profit Function

This figure plots the firm's profit function as stated in (17), where $P_t = 1$ and the aggregate price level in the next period is uncertain and given by either $P_{t+1} = P_t + \sigma$ or $P_{t+1} = P_t - \sigma$ with equal probability. The applied values are $\theta_\mu = 6$, $\phi_P = 163$, and $\beta = 0.994$.

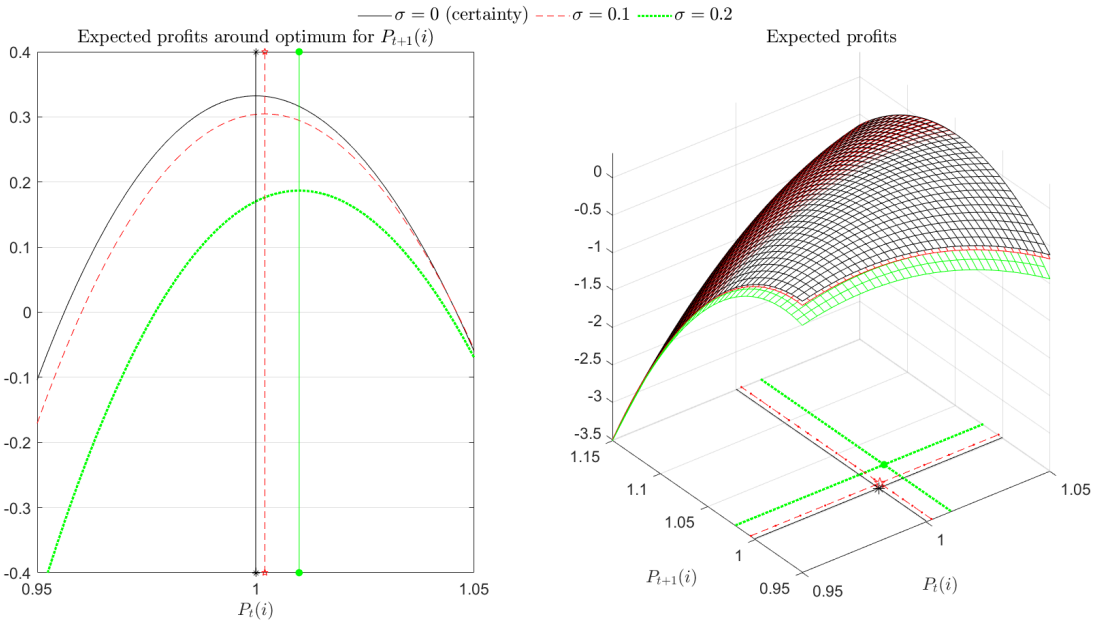

Figure 7 also shows that these pricing biases are increasing in the amount of uncertainty about P_{t+1} - and hence future inflation $\Pi_{t+1} \equiv P_{t+1}/P_t$ - as captured by higher values of σ. This finding is closely related to the result in Born and Pfeifer (2020), who show that higher uncertainty about the aggregate price level generates a higher upward

pricing bias within their static setting. Unreported results also reveal that the pricing biases in $P_t(i)$ and $P_{t+1}(i)$ are increasing for higher values of β, because it increases the importance of the price adjustment costs. Hence, in a more elaborated setting where firms discount profits by a stochastic discount factor, higher values of this discount factor in recessions (due to low consumption and high marginal utility) will increase the pricing bias in $P_t(i)$, and vice versa for expansions with a low discount factor (due to high consumption and low marginal utility).

6.2.2 The Full Model

To understand the determinants behind this state-dependent pricing bias in the full model, let us look at the NKPC which reads

$$\phi_P\left(\frac{\Pi_t}{\Pi_{ss}}-1\right)\frac{\Pi_t}{\Pi_{ss}}=(1-\theta_{\mu,t})+\frac{\theta_{\mu,t}}{\mu_t}+\mathbb{E}_t\left[M_{t+1}\phi_P\frac{Y_{t+1}}{Y_t}\left(\frac{\Pi_{t+1}}{\Pi_{ss}}-1\right)\frac{\Pi_{t+1}}{\Pi_{ss}}\right]. \quad (18)$$

An uncertainty shock enters in this equation through the term with the conditional expectation, i.e., $\mathbb{E}_t\left[M_{t+1}\phi_P\frac{Y_{t+1}}{Y_t}\left(\frac{\Pi_{t+1}}{\Pi_{ss}}-1\right)\frac{\Pi_{t+1}}{\Pi_{ss}}\right]$, which captures the nominal pricing bias. To simplify the interpretation of this term, we show in the Online Appendix that the presence of Y_{t+1}/Y_t does not affect the impulse responses for an uncertainty shock, implying that it is sufficient to study the term $P_t^{\Pi}\equiv\mathbb{E}_t\left[M_{t+1}\phi_P\left(\left(\frac{\Pi_{t+1}}{\Pi_{ss}}\right)^2-\frac{\Pi_{t+1}}{\Pi_{ss}}\right)\right]$. One way to analyze this term is to note that P_t^{Π} is equivalent to the price of a hypothetical asset with pay-off $\phi_P\left(\left(\Pi_{t+1}/\Pi_{ss}\right)^2-\Pi_{t+1}/\Pi_{ss}\right)$. This pay-off increases monotonically for higher values of Π_{t+1} (with slope coefficient $\phi_P\left(2\Pi_{t+1}/\Pi_{ss}^2-1/\Pi_{ss}\right)$), implying that P_t^{Π} represents the price for the firm of buying protection against high inflation in the future. The value of this asset can be decomposed as

$$P_t^{\Pi}=\underbrace{\frac{1}{R_t^R}\mathbb{E}_t\left[\phi_P\left(\left(\frac{\Pi_{t+1}}{\Pi_{ss}}\right)^2-\frac{\Pi_{t+1}}{\Pi_{ss}}\right)\right]}_{\text{Risk-neutral price}}+\underbrace{\mathbb{C}ov_t\left[M_{t+1},\phi_P\left(\left(\frac{\Pi_{t+1}}{\Pi_{ss}}\right)^2-\frac{\Pi_{t+1}}{\Pi_{ss}}\right)\right]}_{\text{Risk premium}}, \quad (19)$$

where $R_t^R=1/\mathbb{E}_t\left[M_{t+1}\right]$ denotes the gross real interest rate. The first term on the right hand side in (19) is the risk-neutral price of this hypothetical asset with its expected pay-off discounted by the real rate. The second term is the additional price that a risk-averse investor is willing to pay for inflation protection and constitutes a risk premium. The unconditional mean of this risk premium is 1.9% in the model, but it displays considerable counter-cyclical variation with a low mean of 0.9% in expansions and a high mean of 3.7% in recessions.

The top row of Figure 8 shows that the asymmetric responses of prices and inflation to an uncertainty shock go hand in hand with the asymmetric response of the price of this hypothetical asset P_t^{Π}. In the bottom row of this figure, we further show that

Figure 8: New Keynesian Model: Determinants of the Upward Pricing Bias
This figure shows the impulse response functions following a positive one-standard deviation uncertainty shock (i.e. $\epsilon_{\sigma,t} = 1$) in the New Keynesian model using the estimates in column (1) of Table 4. The responses are shown for strong expansions and deep recessions. The risk premium in P_t^{Π} is given by $\mathbb{C}ov_t\left[M_{t+1}, \phi_P\left(\left(\frac{\Pi_{t+1}}{\Pi_{ss}}\right)^2 - \frac{\Pi_{t+1}}{\Pi_{ss}}\right)\right]$, the inflation volatility risk premium is defined as $\mathbb{C}ov_t\left[M_{t+1}, \phi_P\left(\frac{\Pi_{t+1}}{\Pi_{ss}}\right)^2\right]$, and inflation volatility is measured by $\mathbb{V}_t\left[\Pi_{t+1}\right]$. The responses of prices and inflation are shown in percentage deviations, whereas the other response are scaled by 100 and shown in absolute deviations.

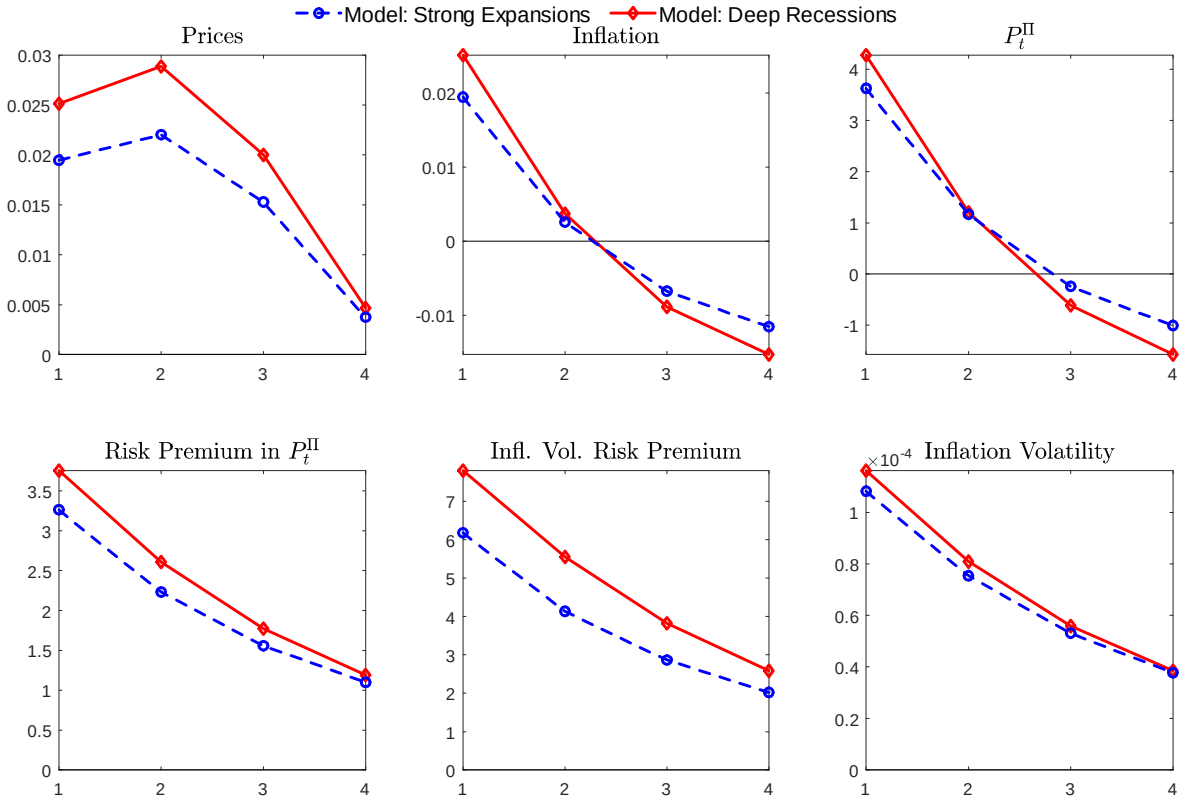

these asymmetric responses in P_t^{Π} are generated by the risk premium. The dominating term in this risk premium is the squared term for inflation, i.e., $\mathbb{C}ov_t\left[M_{t+1}, \phi_P\left(\frac{\Pi_{t+1}}{\Pi_{ss}}\right)^2\right]$, which can be interpreted as an inflation volatility risk premium. To understand why this conditional covariance displays larger responses in recessions than in expansions, we exploit two insights from the simplified two-period setting discussed above.

First, the inflation volatility risk premium is closely related to the amount of inflation volatility, which increases the pricing bias as shown in Section 6.2.1. One way to measure the degree of inflation volatility is to compute the conditional variance of inflation $\mathbb{V}_t\left[\Pi_{t+1}\right]$. We find that the mean of $\mathbb{V}_t\left[\Pi_{t+1}\right]$ in recessions is 19% higher than the mean in expansions, showing that recessions in the New Keynesian model are characterized by much more inflation volatility than expansions.[22] The process for stochastic volatility

[22] This is consistent with empirical evidence, both when measuring inflation volatility by the interquar-

$\sigma_{a,t}$ contributes in two important ways to generate this asymmetry. First, recessions have a higher value of $\sigma_{a,t}$ than expansions, implying that an equal-size preference shock $\epsilon_{a,t+1}$ is expected to have a larger impact on inflation in recessions than in expansions. Second, the bottom right chart in Figure 8 shows that an uncertainty shock increases inflation volatility by more in recessions than in expansions.

Second, another key driver of the inflation volatility risk premium is the dynamics of the stochastic discount factor M_{t+1}. In the New Keynesian model, we find that the realized values of M_{t+1} have a higher level in recessions than in expansions due to lower consumption and higher marginal utility than in expansions. As shown in Section 6.2.1, a higher value of the discount factor increases the weight in the profit function to the intertemporal smoothing of the pricing bias, and as a result helps to generate a larger upward pricing bias in recessions than in expansions.

Thus, the economic intuition behind the state-contingent upward nominal pricing bias is as follows. With price stickiness as in Rotemberg (1982), firms can reset their prices in every period but face costs when doing so. In this multiperiod setting, inflation volatility affects the current price, because it is optimal for firms to set higher prices after an uncertainty shock to avoid large expensive future increases in prices. Two effects help to make this pricing bias stronger in recessions than expansions. First, inflation volatility is higher in recessions than in expansions. Second, firms discount future profits by the stochastic discount factor, which has a higher level in recessions than in expansions. This implies that firms assign more weight to future profits, which also helps to increase their pricing bias by more in recessions than in expansions.

6.3 External Validation of the Key Mechanism

The reduction in real activity following uncertainty shocks implies that wages and the rental rate of capital also fall in the New Keynesian model (not shown). With higher prices, we therefore see a higher price markup, which Fernández-Villaverde et al. (2015) and Basu and Bundick (2017) show is the key driver behind the real effects of uncertainty shocks in the model, although Born and Pfeifer (2020) challenge this effect. Our finding that the upward nominal pricing bias is state-contingent helps to clarify how this channel works across the business cycle. This is illustrated in Figure 9, which shows that the price markup increases by more in recessions than in expansions (top chart to the left), and that this difference disappears when we omit the state-contingent nominal pricing bias (top chart to the right).

Thus, a simple way to validate the key mechanism in the New Keynesian model for generating asymmetric responses to an uncertainty shock is to explore if the price markup

tile range of the one quarter ahead forecast of inflation in the Survey of Professional Forecasts or by a GARCH(1,1) model applied to the residuals of an autoregression with four lags for CPI inflation.

in the US displays asymmetric effects across the business cycle. We implement this external validation of the model by extending the IVAR with the price markup, which we measure by the inverse of the labor share in the business sector as in Fernández-Villaverde et al. (2015). Similar to our baseline analysis in Section 2, we allow the responses of the price markup and the other variables in the IVAR to change across the business cycle. The middle row in Figure 9 reports the median target responses for the price markup in expansions and recessions alone with their 90 percent confidence bands. The responses in recessions are much larger than in expansions, in particular after the first four quarters. This is seen clearly from the bottom left chart in Figure 9, which shows that the median target response in recessions is substantially above the response in expansions. The bottom right chart shows that the differences in these median target responses are significant at the 90% level. Thus, the dynamic responses of the price markup in the US appear to be consistent with the predictions from the New Keynesian model, which leaves further support for the presence of a state-contingent upward nominal pricing bias.[23]

7 Conclusion

This paper employs a nonlinear VAR and a non-recursive identification strategy using a combination of narrative, correlation, and sign restrictions to show that the real effects of an uncertainty shock are stronger when growth is low (as in recessions) than when growth is high (as in expansions). An estimated medium-scale New Keynesian model approximated to third order around the risky steady state goes a long way in reproducing these state-dependent impulse responses to an uncertainty shock. The key mechanism is that firms display a stronger nominal upward pricing bias in recessions than in expansions, as firms face more inflation uncertainty and have a higher value of the discount factor in these states of the business cycle. This leads firms to post higher prices through higher markups in recessions when compared to expansions, which then worsens the real effects of an uncertainty shock in recessions. This prediction is supported by a nonlinear VAR that produces a larger response in an empirical measure of the price markup in recessions than in expansions following an uncertainty shock.

[23] In the Online Appendix, we further show that the only channel that eliminates the state-dependent responses of the price markup to an uncertainty shock is the nominal upward pricing bias channel.

Figure 9: Price Markup

This figure shows the generalized impulse response functions for the price markup in percent to a one-standard deviation uncertainty shock. The top row shows the responses in the baseline New Keynesian model (to the left) and when omitting the nominal pricing bias (to the right) using the estimates in column (1) of Table 4. The charts in the middle row show the median target (MT) reponses in the extended IVAR during strong expansions (to the left) and deep recessions (to the right) along with the 90 % confidence bands. At the bottom row, the differences in the median target responses in the IVAR are reported (to the left), while the difference in these responses between deep recessions and strong expansions are shown to the right along with the bootstrapped 68% and 90% confidence bands.

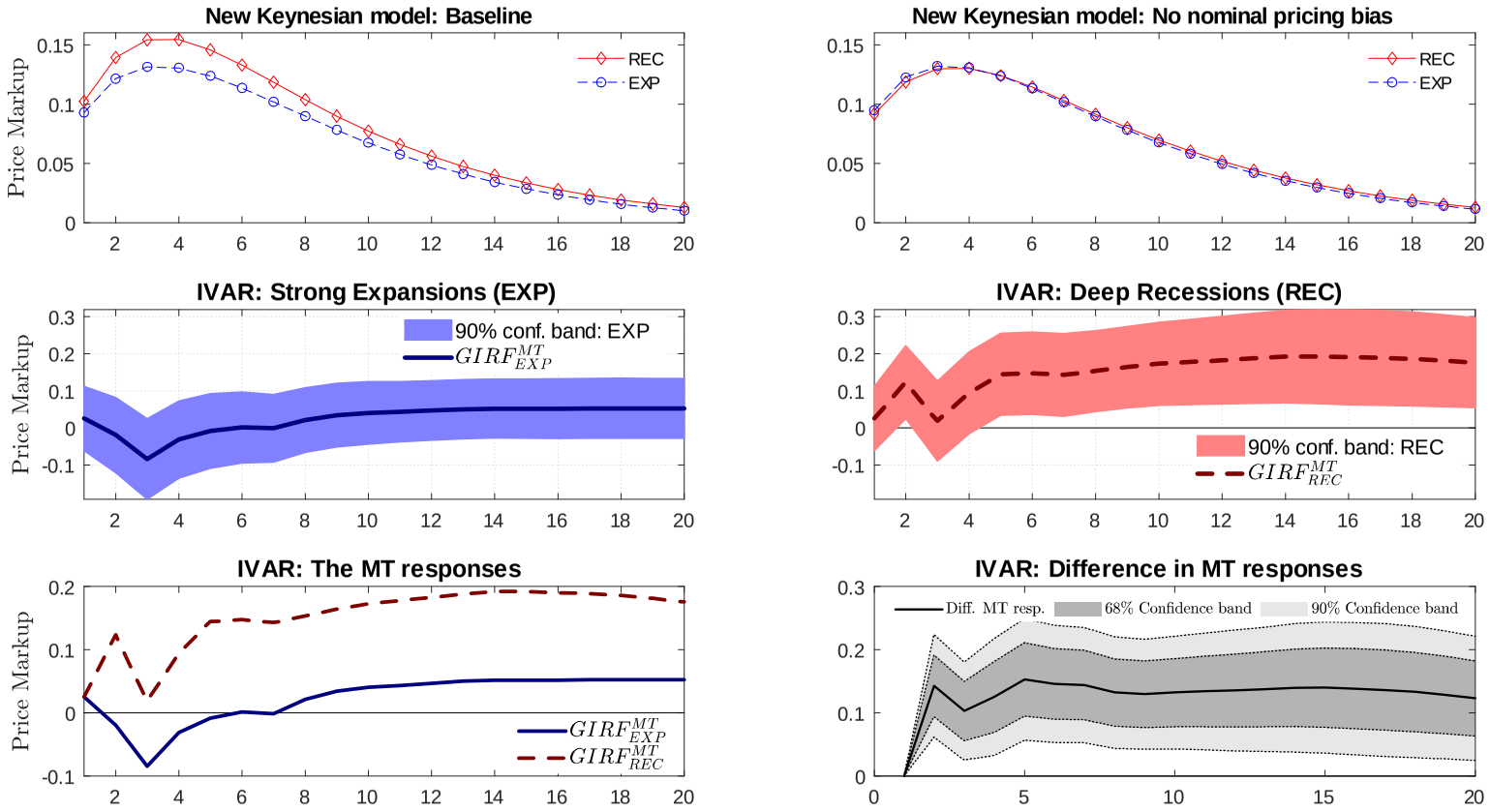

References

Alessandri, P. and Mumtaz, H. (2019), 'Financial regimes and uncertainty shocks', *Journal of Monetary Economics* **101**, 31–46.

Andreasen, M. M. (2012), 'On the effects of rare disasters and uncertainty shocks for risk premia in non-linear dsge models', *Review of Economic Dynamics* **15(3)**, 295–316.

Andreasen, M. M., Fernández-Villaverde, J. and Rubio-Ramírez, J. F. (2018), 'The pruned state-space system for non-linear dsge models: Theory and empirical applications', *Review of Economic Studies* **85(1)**, 1–49.

Andreasen, M. M. and Jørgensen, K. (2020), 'The importance of timing attitudes in consumption-based asset pricing models', *Journal of Monetary Economics* **111**, 95–117.

Antolín-Díaz, J. and Rubio-Ramírez, J. F. (2018), 'Narrative sign restrictions', *American Economic Review* **108**(10), 2802–2829.

Aruoba, S., Bocola, L. and Schorfheide, F. (2017), 'Assessing DSGE Model Nonlinearities', *Journal of Economic Dynamics & Control* **83**, 34–54.

Barrero, J. M. and Bloom, N. (2020), 'Economic uncertainty and recovery', **Jackson Hole Economic Policy Symposium Paper, August**.

Barsky, R., Juster, F., Kimball, M. and Shapiro, M. (1997), 'Preference parameters and behavioral heterogeneity: An experimental approach in the health and retirement study', *Quarterly Journal of Economics* **112(2)**((2)), 537–579.

Basu, S. and Bundick, B. (2017), 'Uncertainty shocks in a model of effective demand', *Econometrica* **85(3)**, 937–958.

Basu, S. and Bundick, B. (2018), 'Uncertainty shocks in a model of effective demand: Reply', *Econometrica* **86(4)**, 1527–1531.

Bianchi, F., Kung, H. and Tirskikh, M. (2019), 'The origins and effects of macroeconomic uncertainty', **Duke University and London Business School, available at https://sites.google.com/view/francescobianchi/home**.

Binning, A. (2013), 'Solving second and third-order approximations to dsge models: A recursive sylvester equation solution', **Norges Bank Working Paper No. 18**.

Binsbergen, J. H. V., Fernández-Villaverde, J., Koijen, R. S. and Rubio-Ramírez, J. (2012), 'The term structure of interest rates in a dsge model with recursive preferences', *Journal of Monetary Economics* **59(7)**, 634Ű648.

Bloom, N. (2009), 'The impact of uncertainty shocks', *Econometrica* **77(3)**, 623–685.

Bloom, N. (2014), 'Fluctuations in uncertainty', *Journal of Economic Perspectives* **28(2)**, 153–176.

Born, B. and Pfeifer, J. (2014), 'Risk matters: The real effects of volatility shocks: Comment', *American Economic Review* **104(12)**, 4231–4239.

Born, B. and Pfeifer, J. (2020), 'Uncertainty-driven business cycles: assessing the markup channel', *Quantitative Economics* **forthcoming**.

Cacciatore, M. and Ravenna, F. (2020), 'Uncertainty, wages, and the business cycle', *Economic Journal* **forthcoming**.

Caggiano, G., Castelnuovo, E. and Groshenny, N. (2014), 'Uncertainty shocks and unemployment dynamics: An analysis of post-wwii u.s. recessions', *Journal of Monetary Economics* **67**, 78–92.

Coeurdacier, N., Rey, H. and Winant, P. (2011), 'The Risky Steady State', *American Economic Review: Papers & Proceedings* **101**(3), 398Ű401.

Collard, F. and Juillard, M. (2001*a*), 'Accuracy of stochastic perturbation methods: The case of asset pricing models', *Journal of Economic Dynamics and Control* **25(6-7)**, 979–999.

Collard, F. and Juillard, M. (2001*b*), 'A higher-order taylor expansion approach to simulation of stochastic forward-looking models with an application to a nonlinear phillips curve model', *Computational Economics* **17(2-3)**, 125–139.

de Groot, O. (2013), 'Computing The Risky Steady State of DSGE Models', *Economic Letter* **120**(3), 566–569.

de Groot, O. (2016), 'What order? perturbation methods for stochastic volatililty asset pricing and business cycle models', **Centre for Dynamic Macroeconomic Analysis Working Paper No. 201606**.

de Groot, O., Richter, A. W. and Throckmorton, N. A. (2018), 'Uncertainty shocks in a model of effective demand: Comment', *Econometrica* **86(4)**, 1513–1526.

Diercks, A. M., Hsu, A. and Tamoni, A. (2020), 'When it rains it pours: Cascading uncertainty shocks', **available at https://andreatamoni.meltinbit.com/**.

Epstein, L. and Zin, S. (1989), 'Substitution, risk aversion, and the temporal behavior of consumption and asset returns: A theoretical framework', *Econometrica* **57(4)**, 937–969.

Fernández-Villaverde, J. and Guerron-Quintana, P. (2020), 'Uncertainty shocks and business cycle research', *Review of Economic Dynamics* **forthcoming**.

Fernández-Villaverde, J., Guerrón-Quintana, P., Kuester, K. and Rubio-Ramírez, J. F. (2015), 'Fiscal volatility shocks and economic activity', *American Economic Review* **105(11)**, 3352–3384.

Fernández-Villaverde, J., Guerrón-Quintana, P., Rubio-Ramírez, J. F. and Uribe, M. (2011), 'Risk matters: The real effects of volatility shocks', *American Economic Review* **101**, 2530–2561.

Fry, R. and Pagan, A. (2011), 'Sign restrictions in structural vector autoregressions: A critical review', *Journal of Economic Literature* **49(4)**, 938–960.

Guerron-Quintana, P. A., Khazanov, A. and Zhong, M. (2021), 'Nonlinear Dynamic Factor Models', *Working Paper* pp. 1–34.

Hamilton, J. D. (2018), 'Why you should never use the hodrick-prescott filter', *Review of Economics and Statistics* **100**, 831–843.

King, R. G., Plosser, C. I. and Rebelo, S. T. (2002), 'Production, growth and business cycles: Technical appendix', *Computational Economics* **20**, 87–116.

Koop, G., Pesaran, M. and Potter, S. (1996), 'Impulse response analysis in nonlinear multivariate models', *Journal of Econometrics* **74(1)**, 119–147.

Levintal, O. (2017), 'Fifth-order perturbation solution to dsge models', *Journal of Economic Dynamics and Control* **80**, 1–16.

Ludvigson, S. C., Ma, S. and Ng, S. (2019), 'Uncertainty and business cycles: Exogenous impulse or endogenous response?', *American Economic Journal: Macroeconomics* **forthcoming**.

Rotemberg, J. J. (1982), 'Monopolistic price adjustment and aggregate output', *Review of Economic Studies* **49**, 517–531.

Rubio-Ramírez, J. F., Waggoner, D. F. and Zha, T. (2010), 'Structural vector autoregressions: Theory of identification and algorithms for inference', *Review of Economic Studies* **77**, 665–696.

Rudebusch, G. D. and Swanson, E. T. (2012), 'The bond premium in a dsge model with long-run real and nominal risks', *American Economic Journal: Macroeconomics* **4(1)**, 105–143.

Salgado, S., Guvenen, F. and Bloom, N. (2019), 'Skewed Business Cycles', *NBER Working Paper* (No. 26565).

Schmitt-Grohe, S. and Uribe, M. (2004), 'Solving dynamic general equilibrium models using a second-order approximation to the policy function', *Journal of Economic Dynamics and Control* **28**, 755–775.

Swanson, E. T. (2018), 'Risk aversion, risk premia, and the labor margin with generalized recursive preferences', *Review of Economic Dynamics* **28**, 290–321.

Weil, P. (1990), 'Nonexpected utility in macroeconomics', *Quarterly Journal of Economics* **105(1)**, 29–42.

Wu, J. C. and Xia, F. D. (2016), 'Measuring the macroeconomic impact of monetary policy at the zero lower bound', *Journal of Money, Credit, and Banking* **48(2-3)**, 253–291.